Delft University of Technology

Designing the Ornicopter, a tailless helicopter with active flapping blades a case study

Wan, Jia; Pavel, Marilena

DOI
10.1177/0954410015622228

Publication date
2016

Document Version
Accepted author manuscript

Published in
Journal of Aerospace Engineering

Citation (APA)
Wan, J., & Pavel, M. (2016). Designing the Ornicopter, a tailless helicopter with active flapping blades: a case study. *Journal of Aerospace Engineering*, *230*(12), 2195-2219. https://doi.org/10.1177/0954410015622228

Important note
To cite this publication, please use the final published version (if applicable).
Please check the document version above.

Copyright
Other than for strictly personal use, it is not permitted to download, forward or distribute the text or part of it, without the consent of the author(s) and/or copyright holder(s), unless the work is under an open content license such as Creative Commons.

Takedown policy
Please contact us and provide details if you believe this document breaches copyrights.
We will remove access to the work immediately and investigate your claim.

This work is downloaded from Delft University of Technology.
For technical reasons the number of authors shown on this cover page is limited to a maximum of 10.

Designing the Ornicopter, A Tailless Helicopter with Active Flapping Blades - A Case Study

Jia Wan, Marilena D. Pavel

Abstract

The Ornicopter concept is a single rotor, tailless configuration. By actively flapping its blades, the Ornicopter rotor can propel itself to rotate, and hence does not need a tail rotor. In previous research, the Ornicopter concept has been compared with the Bo-105 conventional helicopter from various aspects, while the Ornicopter has the same design parameters as the Bo-105. Comparisons show that the Ornicopter has one major drawback, namely a small flight envelope. To improve the Ornicopter performance and understand how the Ornicopter should be designed, in this paper, the Ornicopter design is unfrozen and optimized for flight envelope. The optimization result shows that with a proper design, the Ornicopter performance can be improved dramatically. A similar flight envelope as the Bo-105 can be achieved for the Ornicopter. However, the Ornicopter requires higher power than the Bo-105 due to the inherent characteristics of this concept.

Keywords

Ornicopter, tailless, conceptual design, performance

Introduction

General background

Among the large number of helicopters, the single main rotor/tail rotor (conventional) configuration is the main configuration in use today. The configuration of a helicopter is, to a large extent, determined by the manner in which the reaction torque of the main rotor is counteracted. For conventional helicopters, the tail rotor is used for this purpose, as well as for generating yaw control.

Although the tail rotor gives the helicopter extreme manoeuvrability, it also has many unfavourable characteristics: it consumes power, and has only marginal control authority under unfavourable wind conditions; it is noisy, vulnerable and dangerous. Research has shown that about 50% of U.S. civil helicopter accidents related to airframe failure or malfunction between 1963 and 1997 are connected to the tail rotor system (including the drive train, control system, tailboom and tail rotor) [1].

Different solutions have been proposed in an attempt to solve the shortcomings of the classical tail rotor system. Some configurations have been successfully developed and implemented, such as: the Fenestron system, the NOTAR system (NO TAil Rotor), the tandem helicopter, the coaxial helicopter and the synchropter (intermeshing rotors) configuration.

Inspired by birds, efforts have been made to invent a flapping wing aircraft (also known as an ornithopter). The flapping wing concept can also be applied to the rotary-wing aircraft in order to design a tailless helicopter. Previous attempts to design a flapping blade helicopter go back in to 1930s. Two devices were patented by Hans Georg Küssner, a German aerodynamicist, at the 'Gottingen Aerodynamic Test Establishment' [2, 3]. His invention, the so-called 'Flapping Propulsion Rotor', was based on the flapping blades concept. In his patent, the flapping actuation device was based on an oil-hydraulic pump system to simultaneously flap up and down a pair of centrally hinged rotor blades [2]. In order to demonstrate his concept, Küssner also developed a wind tunnel model, and showed experimentally that the reaction torque could be completely compensated for by the rotating flapping blades in such a concept.

At the end of the 1990s, Dr. Vladimir Savov from the Bulgarian Air Force Academy proposed the so-called 'Rotopter' concept [4], using the same principle of the forced flapping blades in order to eliminate the tail rotor. A mechanism was de-

Department of Control and Operation, Faculty of Aerospace Engineering, Delft University of Technology, The Netherlands

Corresponding author:

Jia Wan, Department of Control and Operation, Delft University of Technology, Kluyverweg 1, Delft,2497 XA, the Netherlands

Email: williamwanjia@gmail.com

signed and patented by Savov, the so-called 'freewheeling flapping wing'. Its blades can rotate freely and are forced to flap around the flapping hinge by the crank-rod mechanism. This flapping motion generates the propulsion force to drive the rotor to rotate.

In 2002, Delft University of Technology proposed the 'Ornicopter' configuration as an alternative manner to eliminate the tail rotor. The main idea behind the Ornicopter is that, instead of counteracting the rotor torque, it is better to use a rotor concept that does not generate a torque.

The name 'Ornicopter' came from the combination of 'Ornithopter' and 'Heli-copter'. As its name suggests, the Ornicopter can be considered as a helicopter version of the Ornithopter, the aircraft that flies like a bird by flapping its wings.

In conventional helicopters, the rotor blades are driven by the shaft torque to rotate, and they generate lift from this rotating motion. This will cause a reaction torque on the fuselage that needs to be compensated for by an anti-torque device. In the case of the Ornicopter, the blades flap in the same manner as a bird and derive both lift and propulsive force from this movement. Thus, the Ornicopter combines the flapping wing principle with the helicopter principle. As the blades propel (i.e. rotate) themselves, there is no longer a need for a direct torque supplied by the engine to rotate the blades. Therefore, the Ornicopter rotor will not generate a reaction torque on its fuselage. This makes the anti-torque device redundant.

At Delft University of Technology, some research related to the Ornicopter has been performed. Initially, the basic Ornicopter principle was proposed, followed by feasibility analyses based on an analytical model for the Ornicopter rotor in hovering condition [5]. The principle of how to achieve the forced flapping motion on the Ornicopter was also defined later on [6, 7].

Three rotor configurations for the Ornicopter have been proposed [8], including the double-teeter configuration, the 2×2 anti-symmetrical configuration (referred as 2×2 AS in what follows), and the so-called the 3-in-1-plane configuration. Due to the relatively low vibration loads, the 2×2 AS has been chosen to be the basic flapping configuration of the Ornicopter. As shown in Fig. 1, when a blade ($k = 0$) is flapping upwards, the opposite blade ($k = 2$) is flapping upwards as well, while at the same time the two other blades will be flapping downwards, and vice versa. The blades will pass through the neutral position at the same moment in time.

In 2004 flapping mechanisms were developed in practice [8] and tested on a small wind tunnel test model, as well as an Ornicopter demonstrator model. A new mechanism was patented by

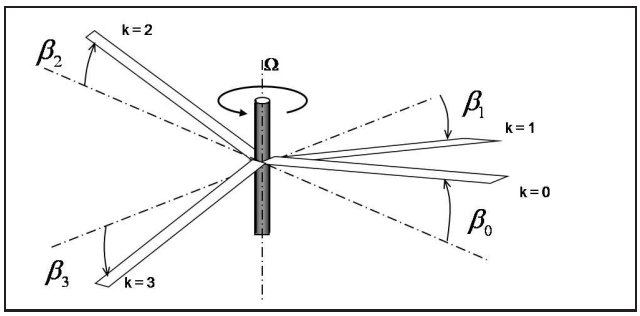

Figure 1: Principle of the 2×2 AS configuration [8]

Prof. Theo van Holten [9] in 2004 as shown in Fig. 2. The second swashplate, the so-called 'force-flapping swashplate' was added to the Ornicopter rotor. The rotating push rod will be driven by this swashplate to move up and down when the rotor is rotating, and hence drives the blade to flap.

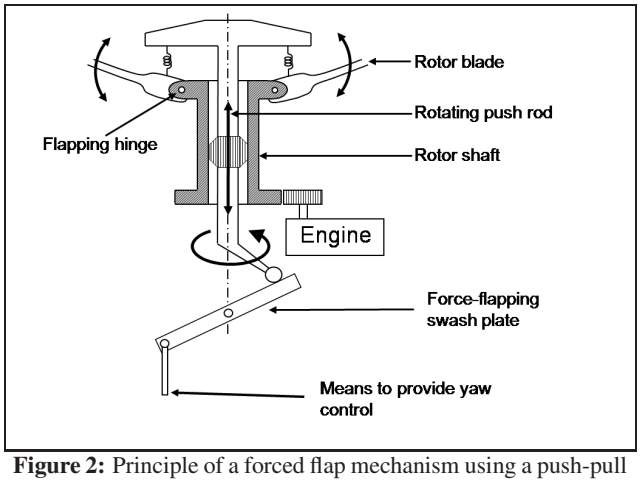

Figure 2: Principle of a forced flap mechanism using a push-pull rod and swashplate [9]

Since 2009, more detailed research has been performed for the Ornicopter concept. A flight mechanics model is developed for this concept based on the blade element theory [10] , and is validated against some test data in the hovering condition [11]. This model includes the body motion dynamics, blade flapping dynamics and inflow dynamics. Using this model, the Ornicopter was compared with the benchmark helicopter (Bo-105). The Ornicopter calculations were made assuming that it is in the range of a light-weight helicopter and using the same initial design parameters as Bo-105 helicopter (see Tab. 1). Figure 3 gives a sketch of a possible Ornicopter design using the 2×2 AS configuration [12].

Different aspects are considered during the comparisons, namely the performance [11, 13], stability and controllability [11, 14], and handling qualities [15]. Those comparisons are performed for both hovering and forward flight conditions to understand the impacts of eliminating the tail rotor and the additional active flapping on helicopters. The drawbacks of the Ornicopter

concept have been pinpointed, including a small flight envelope and worse stability and handling qualities in yaw direction, while the former one is the major disadvantage of the Ornicopter concept.

Table 1. Main design parameters of the Bo-105

Rotor radius	4.91 m	Blade chord	0.27 m
Solidity	0.07	Disk loading	29.05 kg/m^2
Tip velocity	218 m/s	Rotor RPM	424
Number of blades	4	Gross weight	2200 kg
Tail rotor radius	0.95 m	Length	11.86 m

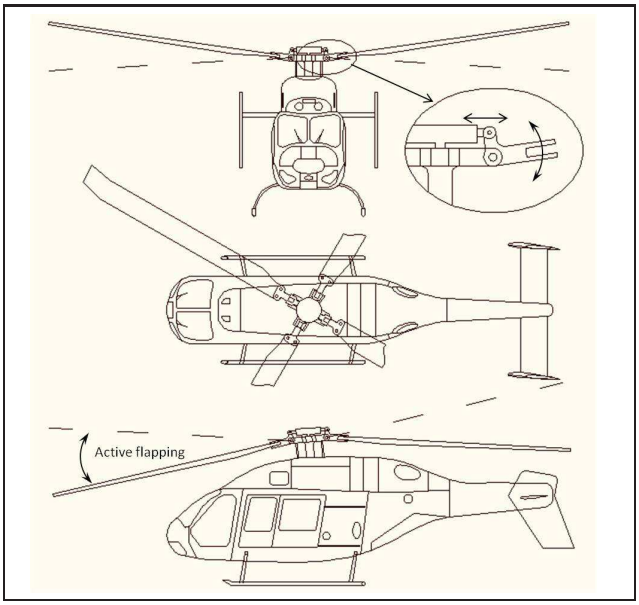

Figure 3: Sketch of a possible Ornicopter design [12]

Goal of the paper

One of the reasons causing these drawbacks of the Ornicopter is that it has the same design as the Bo-105. These design parameters are not optimized for the Ornicopter concept. A simple test design case, i.e. a new design using larger chord length, tip velocity and vertical fin size, has been analyzed [13]. It shows a large improvement in the Ornicopter flight envelope.

In this sense, to further understand the pros and cons of the Ornicopter concept, some design parameters will be unfrozen and optimized to improve the Ornicopter's performance. Afterwards, the optimized design will be compared with the Bo-105 to answer the question that how can an Ornicopter be designed, which has comparable or improved flight performance as compared to the Bo-105.

As an initial attempt to design an Ornicopter, the power requirement and rotor stall area will be the main interest in this paper. Some more advanced effects, such as blade elasticity, unsteady aerodynamics and weight variation caused by changing design parameters, are considered at this stage.

A design optimization methodology is presented in this paper related to Ornicopter in order to improve its major drawbacks, i.e. the small flight envelope and the low yaw stability. The design optimisation process uses the following steps. ***

First, a baseline Ornicopter design similar to the Bo-105 helicopter is modelled. A dynamic flight simulation framework of the Ornicopter design is set up to determine its performance characteristics. The sensitivity of different performance criteria (such as required power and stall area) to basic helicopter design parameters was established by varying each parameter in the defined design space. ***

Second, a design space is created for the Ornicopter by varying different helicopter conceptual design parameters (such as rotor radius, blade area, rotor tip speed, fin size, pitch-flap coupling) within the practical constraints that must be imposed on design parameters. For example, minimum tip speed is given by the one corresponding to an advance ratio of 0.5 while maximum tip speed is given by the advancing blade tip Mach number of 0.95. For each design in this design space, calculations of the required power and stall area are performed for two flight conditions: hovering and 120 kts. ***

Third, by analysing the performance data in the design space, the design trends of Ornicopter can be unmasked. Afterwards, those trends are used to define an optimization objective with cost functions and constraints to obtain the final Ornicopter design. ***

Since a model by definition is a simplified representation of reality, uncertainties in predictions of Ornicopter behaviours can result in uncertainties in the design space. However, the model used to predict the Ornicopter's behaviour is suitable in its assumptions to perform parametric trends studies for performance and flying qualities within vehicle's operational flight envelope. Therefore, the uncertainties in the design trends are suited for the analysis of Ornicopter within its operational flight envelope. One can thus assume that the optimized final Ornicopter design obtained in this paper is capable of improving the limited flight envelope of the original design. The new design has a better altitude performance at low speed and fast forward flight, while having lower maximum speed due to the higher required power. ***

***

The Ornicopter concept

The vanished reaction torque

As stated previously, the Ornicopter flaps its blades like a bird. When a bird is flying, both a propulsive force - that pushes the bird to fly through the air - and a lift force - that will keep the bird airborne - are generated by its flapping wings. Similarly, when the blades of a rotating rotor are actively flapping, both a lift force and a propulsive force are generated. In this case, the propulsive force will drive the rotor to rotate.

A very useful and simple understanding of how one can generate propulsive force with an Ornicopter blade is obtained by applying a constant pitch angle to the flapping blade. The movement of an Ornicopter blade during one revolution is illustrated in Fig. 4. During one revolution of the rotation, the blade will be forced to flap both up and down once, resulting in the undulating path shown in Fig. 4.

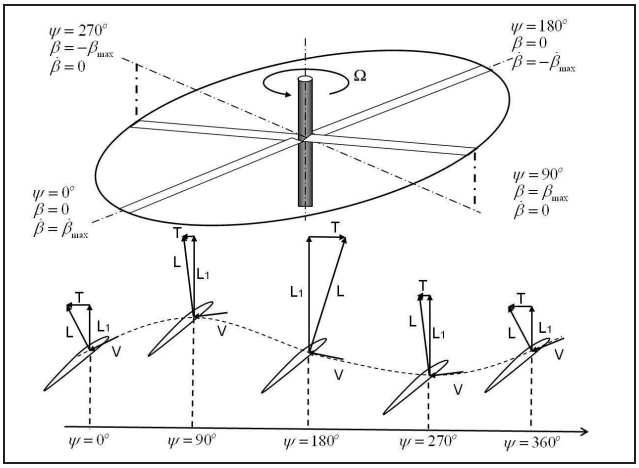

Figure 4: Lift and drag forces acting on an Ornicopter blade during one revolution when a constant pitch angle is applied

At 0° azimuth angle (ψ), the blade element passes through the neutral position with maximum upwards velocity. Due to the upwards flapping velocity, the overall speed (V) will rotate upwards, and hence the angle of attack of the blade element will decrease, resulting in relatively low lift force (L). At the same time, the lift force, which is perpendicular to the relative air flow vector, will follow the change of the incoming wind direction. Therefore, it tilts backwards with regard to the blade element.

After 90 degrees the blade reaches the maximum flapping deflection, where the flapping velocity is zero. The total velocity of the blade element is parallel to the flow direction as in the case without flapping, i.e. as a normal helicopter blade. A similar situation can also be found when the blade reaches 270°. On the contrary, the blade reaches negative maximum flapping deflection at 270° azimuth angle.

Between 90° and 270°, the blade flaps downwards. In contrast to the upwards flapping discussed above, when the blade flaps down, the angle of attack of the blade element will increase, and the increased lift force will tilt forward with regard to the blade element. This results in a positive thrust force, by which the blade is propelled.

When a constant pitch angle is applied, the lift forces during one revolution will (averaged over one revolution) result in an upwards force and an average propulsive force. This average propulsive force is achieved because the forward horizontal component of the lift force that occurs when the blade is flapping downwards (from 90° to 270°) is much larger than the backwards horizontal component of the lift force that occurs when the blade is flapping upwards (from 0° to 90° and 270° to 360°). Thus, by setting all the Ornicopter blades at a constant pitch angle and flapping them up and down, a propulsive force is created that will rotate the blades around the rotor hub and an upwards force is created that will counteract gravity. The amount of propulsion force and the total thrust generated by the rotor are determined by the amplitude of flapping motion and the blade collective pitch. By choosing a proper combination of these two parameters, the desired forces can be achieved for trimmed flight or necessary control.

When the blades are propelled by a flapping motion one can demonstrate that the reaction torque acting on the fuselage will no longer exist. This can be explained by comparing a conventional helicopter to an Ornicopter, see Fig. 5 [6]. In a conventional helicopter the drag that acts on the rotor blades is counteracted by the shaft torque, which drives the rotor to rotate (see Fig. 5.a). As a result, there will also be a reaction torque from the rotor on the fuselage, and this reaction torque will have to be counteracted by an anti-torque device. For the Ornicopter configuration, the drag that acts on the rotor blades is counteracted by the propelling force produced by the forced flapping motion of the blades (see Fig. 5.b). There is thus no direct torque transferred from the fuselage to the rotor to rotate the blades. As a consequence, there will not be a reaction torque from the rotor on the fuselage. Hence, an anti-torque device is no longer necessary.

It should also be mentioned that, for the Ornicopter design, the blade flapping motion has to be synchronized with the rotational speed of the rotor. In this manner, the forced flapping frequency can be kept close to the natural frequency of the blade flapping motion. Due to the resonance effect, the forced flapping motion can reach the maximum amplitude. In other words, in this situation, the minimum driving moment is needed for the ***

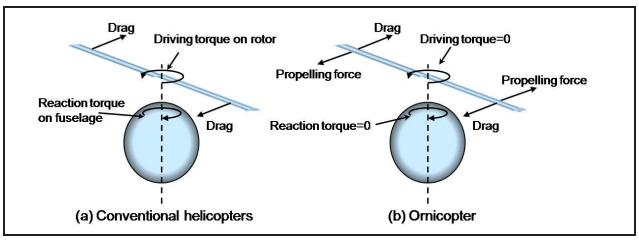

Figure 5: The forces and moments acting on a conventional helicopter and the Ornicopter [6]

forced flapping.

Controlling the Ornicopter

Yaw control. In a conventional helicopter, yaw control is realized by the tail rotor. By increasing or decreasing the thrust of the tail rotor, the total yawing moment on the fuselage can be controlled. Since the Ornicopter obviously does not have a tail rotor, a different means for yaw control is needed.

By introducing a small amount of change in the forced flapping amplitude, the propelling force generated by the Ornicopter rotor can be controlled in order to achieve the desired yaw control moment. From Fig. 4, it can be seen that the propelling force is related to the amplitude of the plunge motion. By increasing the amplitude of the plunge motion (increasing h), the velocity of the vertical motion can be increased, which causes a higher effective angle of attack and larger thrust force. Similarly, the propelling forced generated by the Ornicopter rotor can also be decreased when lower amplitude of the forced flapping is applied. In this manner, the Ornicopter can be controlled in the yaw direction, as shown in Fig. 6.

Figure 6.a presents the case when no yaw movement is desired (the flapping mechanism will be explained later). In this case the blades of the Ornicopter will be entirely propelled by blades flapping, and there will thus be no reaction torque acting on the fuselage. To realize this reactionless situation, a particular amplitude of the forced flapping motion will be necessary. All the engine power will be converted into the flapping of the blades.

When, for the same situation, a small reduction of the flapping amplitude is chosen (Fig. 6.b), the propelling force generated by the active flapping will also be reduced. This implies that the flapping of the blades will not be sufficient to keep the rotor at its required rotational speed (the rotor will tend to slow down), and therefore some additional shaft torque will be needed. The same engine power is now used both for flapping of the blades and for applying some additional shaft torque. Since in this the case shaft torque is directly transmitted from the fuselage to the

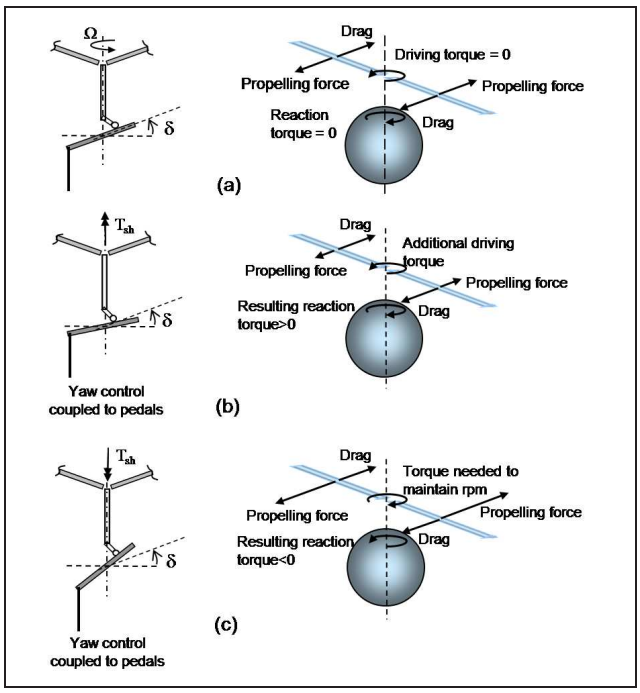

Figure 6: Schematic representation of yaw control by introducing a reaction torque

rotor, there will also be a reaction torque acting on the fuselage. This reaction torque will cause yawing.

To yaw in the opposite direction, a larger amplitude of forced flapping motion of blades needs to be applied (Fig. 6.c). As a result of the larger flapping motion of the blades, the propelling force will increase and as a result the rotor will tend to speed up. In order to keep the rotor at its desired rotational speed, the rotor will have to be slowed down. The reaction torque caused by this is acting in the opposite direction as is the situation in Fig. 6.b, and will therefore cause a yaw movement in the opposite direction, as shown in Fig. 6.c.

Cyclic and collective control. The cyclic and collective controls for the Ornicopter are the same as those for conventional helicopters. A normal swashplate is used in the Ornicopter drive train. Using this conventional swashplate, the pitch angle of the blades can be controlled as per a conventional helicopter. ***

As each blade is forced to flap, their tip-path planes will be tilted in a certain direction according to the forced flapping moment. To minimise additional hub shears and moments, the average tip-path plane of all the blades should not be changed by the forced flapping motion. One possible way is to drive blades anti-symmetrically, as shown in Fig. 7.a [7]. These two tip-path planes tilt in opposite directions to maintain the average tip-path plane level. When the cyclic pitch control is applied, the tip-path planes of all the blades will tilt in the same way, as shown in Fig. 7.b. This is true for both the Ornicopter and normal heli-

copters.

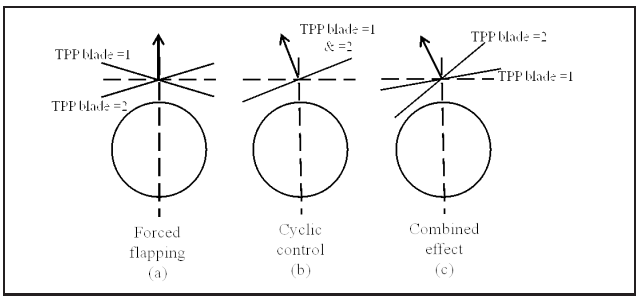

Figure 7: Cyclic control of Ornicopter [7]

It can thus be seen that each swashplate has a different effect on the tip-path planes of the blades. The combination of these two effects results in the total effect, as depicted in Fig. 7.c. Increasing the forced flapping angle and applying cyclic control are two effects that can be superimposed. Cyclic control can be achieved on top of the forced flapping motion and independent of the magnitude of this forced flapping motion. The required cyclic control is thus not influenced by the forced flap and subsequently not influenced by the yaw control. In other words, there is a complete mutual decoupling of the cyclic and yaw control. In this manner, longitudinal and lateral control of the Ornicopter can be achieved.

As in conventional helicopters, a coupling does exist between collective control and yaw movement. If collective control is applied, the pitch angle of all the blades will increase, thereby providing more lift and also more drag. This increase in drag will tend to slow the rotor down, and thus some additional engine power will have to be transferred directly to the shaft. This causes a reaction torque which will cause the fuselage of the Ornicopter to yaw. This problem can be solved in exactly the same way as in conventional helicopters by applying yaw control in the opposite direction; however, instead of requiring a change in pitch angle of the tail rotor blades when the collective is used, in the Ornicopter configuration a change in the forced flapping angle is required. As a result the rotor will remain reactionless.

In conclusion, the Ornicopter changes the means of yaw axis control when compared to a conventional helicopter. In this new configuration, control of all axes is achieved through the main rotor.

The small flight envelope of Ornicopter

The flight envelope is the closed area in the altitude-velocity diagram, in which steady state flight is possible. It is determined by a large number of factors, such as weight, aerodynamics, engine system, structural dynamics and atmospheric conditions [16]. For the preliminary flight envelope prediction, simplified criteria are used in this paper, including the power requirement and stall area.

Power criterion. To analyse the altitude performance of the Ornicopter, an engine model is required to predict the available engine power at different altitudes. As the main purpose of this analysis is to compare the performance of the Ornicopter and Bo-105 instead of to acquire accurate performance data, a simple engine model is used, [16]: ***

$$P_e \approx P_{e_0}\sigma_\rho^{1.35} \tag{1}$$

where P_e is the available engine power, P_{e_0} is the available engine power at sea level and σ_ρ is the relative air density.

Inside the flight envelope, the engine should provide not only the required power for steady flight, but also some power margin for manoeuvrability. Therefore, the power criterion for each flight condition can be defined as:

$$P_0 \leq k_p P_e \tag{2}$$

where P_e is the maximum continuous power available from the engine in each flight condition, P_0 is the total required power of helicopters and k_p is the power margin factor considering the manoeuvrability margin and transmission loss.

In this paper, the k_p is determined through an empirical way based on the Bo-105 specifications and model calculations. The required power of the Bo-105 at maximum velocity (sea level) is calculated using flight mechanics model and compared with the available engine power to determine the k_p, as:

$$k_p = \frac{P_0|_{V_{max}}}{P_{e_0}} \approx 0.846 \tag{3}$$

Stall criterion. The effects of stall affect the performance of helicopters, e.g. the increase control loads and decrease control authority. For the preliminary Ornicopter analyses, a relatively simple criterion is defined based on the nondimensional total stall area ($\bar{S}$):

$$\bar{S} = \frac{S_{stall}}{\pi R^2} \leq \bar{S}_{max} \tag{4}$$

where S_{stall} is the average stall area of all the blades, R is the rotor radius and $\bar{S}_{max}$ is the non-dimensional stall area boundary.

Similarly to the k_p, the stall boundary ($\bar{S}_{max}$) is also determined through the stall area prediction of the Bo-105 at maximum speed, as:

$$\bar{S}_{max} = \frac{S_{stall}|_{V_{max}}}{\pi R^2} \approx 8.93\% \tag{5}$$

Flight envelopes of the Ornicopter and Bo-105. With the criteria defined above (Eq. 2 and 4), the flight envelopes (altitude vs. velocity) of the Ornicopter and Bo-105 are calculated and presented in Fig. 8. Two boundaries are drawn separately to show more details about the different characteristics of the Ornicopter and Bo-105.

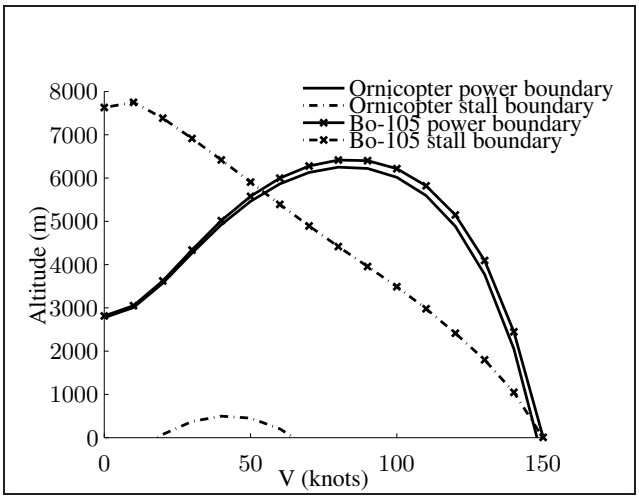

Figure 8: Flight envelope of the Ornicopter and Bo-105 defined by different criteria

From Fig. 8 one can see that the boundaries determined by the power requirement for the Ornicopter and Bo-105 are very close to each other, due to the similar power required by both helicopters. The Ornicopter needs slightly more power than the Bo-105, and therefore the power boundary of the Ornicopter is slightly smaller than that of the Bo-105.

The interesting difference corresponds to the stall boundaries. It can be found that the Ornicopter has a much smaller flyable region when compared to the Bo-105. This is due to the high stall area in both hovering and forward flight. The stall area of the Ornicopter and Bo-105 rotors at two altitudes (sea level and 2000 m) is presented in Fig. 9.

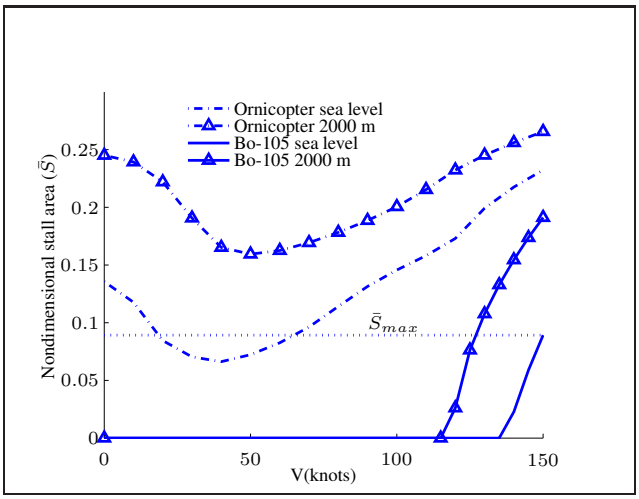

Figure 9: The rotor stall area of the Ornicopter and Bo-105 versus velocity

In forward flight, due to the blade longitudinal flapping and the longitudinal cyclic pitch control, stall occurs on the retreating side of the rotor. In the Ornicopter case, the additional active flapping motion enlarges the stall area of the Ornicopter rotor. Therefore, stall reaches the stall boundary earlier (around 65 knots) on the Ornicopter rotor than the Bo-105, as shown in Fig. 9.

Figure. 8 also shows that in hovering, the Bo-105 hovering ceiling is decided by the required power, while in the case of the Ornicopter, the stall effect is the most limiting factor. The stall area on the Ornicopter rotor is higher than the stall limitation in hovering at sea level, and increases with increasing altitude, as shown in Fig. 9.

In hovering flight, when the altitude is increasing, the air density decreases, and hence the induced velocity increases for the same rotor thrust. In this sense, higher collective pitch is needed, since higher induced velocity results in a lower angle of attack of the blade element and higher induced power. However, the total effect on the blade elements is only a slightly higher AoA. The AoA, and hence stall area, increase slowly with increasing altitude of the conventional helicopter rotor. Therefore, for conventional helicopters, the stall area will not reach the stall limitation in hovering until a very high altitude.

For the Ornicopter, some parts of its rotor encounter stall in hovering due to active flapping. The stall area is correlated with the amplitude of forced flapping motion. Recalling the trim values of the Ornicopter presented before, the yaw control input has a typical bucket shape. This results in similar bucket shape cures for the Ornicopter stall area as a function of velocity, as shown in Fig. 9.

To conclude, due to the active flapping, the blade angle of attack varies in a large range for the Ornicopter rotor, and hence causes a large stall on the rotor of Ornicopter. This stall effect degrades the Ornicopter performance dramatically in terms of the flight envelope.

Design requirements and methods

Due to the active flapping and the absence of a tail rotor, two major drawbacks of the Ornicopter are found in the previous research, including a small flight envelope and low yaw stability and handling qualities. Because it is a first attempt to optimize the Ornicopter design, the handling qualities will not be considered as design requirements in this paper. The performance is the main interest of the Ornicopter design process. In this sense, the flight envelope of the Bo-105 (as predicted in Fig. 8) will

be used as the design requirements of the Ornicopter. The main performance specifications are summarized in Tab. 2.

Table 2. Bo-105 performance predicted by Delcopter

Hovering ceiling	Service ceiling	Max. velocity
2815 m	5725 m	150 knots

To predict the flight envelope of a helicopter, a numerical method needs to be used to search the boundaries of flyable region in the altitude-velocity diagram, i.e. analyses need to be performed at multiple altitudes and velocities. This requires high computational power, especially in the optimization process.

To reduce the calculation cost, not the entire flight envelope boundary of the Ornicopter will be calculated for the design optimization. Two specifications will be considered, including the hovering ceiling and the maximum velocity. First, the Ornicopter design will be optimized based on this simplified requirement. Afterwards, the entire flight envelope of the new Ornicopter design will be calculated and compared with the Bo-105 to verify if the design matches the design requirement.

The following procedure will be used for the Ornicopter design:

1. A sensitivity analysis will be performed with regard to design parameters. This is done in order to pinpoint important parameters for the Ornicopter design and their influences on Ornicopter performance.

2. Based on the parameters selected, a design database will be created which contains a large number of Ornicopter designs. Using the database, the general trend of a feasible Ornicopter design will be analyzed.

3. The optimization problem for the Ornicopter will be defined and optimal designs will be attained.

4. The optimized design of the Ornicopter will be compared with the Bo-105 design to verify if it matches the design requirements.

The detailed design of the forced flapping mechanism for full-scale helicopters has not been considered. It is difficult to estimate the weight of these mechanisms accurately at this stage. Therefore, it is assumed that the forced flapping mechanism has the same weight as the tail rotor system, i.e. the Ornicopter has the same gross weight as the Bo-105. This assumption introduces some error for the weight of the Ornicopter. However, it is considered to be negligible.

It should be mentioned that the Ornicopter design in this paper is the initial concept design. This design process is based on the initial estimation of the total weight of the Ornicopter, which is the same as the Bo-105 helicopter. After a new Ornicopter design has been obtained, the weight of Ornicopter should be recalculated to verify whether all the design requirements are satisfied. Multiple iterations of the design process might be needed before the final converged design result is acquired.

The main purpose of the Ornicopter design research in this paper is to trace the general design trends of this new concept and further understand its characteristics compared with a conventional helicopter. The initial design process can provide a relatively good result for this purpose. In this sense, the following design process will not be looped for the final converged result. The weight estimation for the Ornicopter is not considered in this paper. The influence of varying design parameters on the gross weight of the Ornicopter is neglected, i.e. the Ornicopter total weight is assumed constant.

The design parameters

Rotor sizing

The main rotor is the most important component of the helicopter. Proper design of the rotor is critical to meet the performance requirements for the helicopter as a whole. The Ornicopter introduces the additional flapping motion to the rotor, and hence leads to different characteristics for the Ornicopter as discussed before. In this sense, the main rotor design will be the main concern of the Ornicopter design research in this paper.

The conceptual and preliminary design of the main rotor generally encompasses the following parts [17]:

1. The general sizing, i.e. the rotor diameter and the rotor tip velocity.

2. The geometric platform of the blade which includes the chord, solidity, number of blades, blade twist and tip shape.

3. The choice of airfoil(s).

In this paper, only the general sizing and the blade chord will be discussed as this is decisive for the performance. Other main rotor design elements will be kept constant, such as the number of blades and blade twist.

It should be mentioned that some parameters for the helicopter rotor are correlated to each other. Two sets of them will be presented before the sensitivity analysis, and these are:

1. Rotor radius, tip velocity and rotor rotational speed, as:

$$V_t = R\Omega \tag{6}$$

2. Rotor radius, solidity and blade area, as:

$$\sigma = \frac{A_b}{\pi R^2} \tag{7}$$

In the following research, the rotor radius R, tip velocity V_t and blade area A_b are chosen as design variables. In this sense, the rotational speed Ω and solidity σ will not be constant and vary according to the three chosen design variables.

Vertical fin

The small flight envelope of the Ornicopter is mainly due to the stall, which is directly related to the average AoA and the variation of the AoA on blade elements. In forward flight, the vertical fin design can be modified to reduce the rotor stall area, and hence improve the performance of the Ornicopter.

The oscillation amplitude of the AoA is determined by both the 'conventional' flapping and the forced flapping motion of blades. The latter one is required to balance the rotor shaft torque. In hovering condition, the rotor shaft torque needs to be compensated entirely by the active flapping to reach the reactionless condition. However, this is not necessary in the forward flight, when the vertical fin can generate a yaw moment to compensate for the reaction torque on the fuselage. In this sense, the active flapping of blades only needs to compensate a part of the rotor shaft torque.

When a larger fin size (S_{vs}) and/or a higher incidence angle (β_0^{fin}) is used, the fin can generate higher yaw moment in forward flight, especially at high velocity. In this case, the active flapping motion needs to compensate for a smaller partition of the shaft torque, and hence the forced flapping motion can be reduced, which results in a smaller stall area on the rotor. In this manner, the Ornicopter performance can be improved.

In the steady forward flight condition, the sidewards velocity (v) is very small and the rotational velocities (p, q, r) are zero. Therefore, the yaw moment generated by the vertical fin can be simplified as:

$$N_{fin} = \frac{1}{2}\rho u^2 S_{fin} C_{L_\alpha}^{fin} \beta_0^{fin} x_{fin} \tag{8}$$

Defining the equivalent fin area, as:

$$S_e = S_{fin}\beta_0^{fin} x_{fin} \tag{9}$$

gives the yaw moment generated by the vertical fin as:

$$N_{fin} = P_{dyn} S_e C_{L_\alpha}^{fin} \tag{10}$$

where P_{dyn} is the dynamic pressure ($P_{dyn} = \frac{1}{2}\rho u^2$).

One can see that in steady forward flight the moment generated by the vertical fin is proportional to the equivalent fin area. For different fin designs which have a different fin size (S_{vs}), incidence angle (β_0^{fin}) or fin location (x_{fin}), the yaw moment generated will be the same in steady forward flight, as long as they have the same equivalent fin area. In this sense, the equivalent fin area will be considered as a main design parameter in the sensitivity analysis. To keep it simple, only the fin area will be varied next.

Pitch flap coupling

In the basic Ornicopter concept, the Ornicopter blades are forced to flap with a constant pitch angle. Meanwhile, all the examples of flapping-wing propulsion in nature combine pitching and flapping motions. The combined pitch-plunge flapping wing has been studied in the flapping wing community and research shown that the flapping wing thrust efficiency can be increased by using a combined pitch-plunge motion [18]. Therefore, pitch-flap coupling should also be considered for the Ornicopter concept. It is modeled by two coupling terms as shown in Eq. 11, and their effects on the Ornicopter design will be analyzed. ***

$$\theta = \theta_0 + \theta_{s1}\sin\psi + \theta_{c1}\cos\psi + \theta_{tw}\frac{r}{R} + k_{\theta 1}\beta + k_{\theta 2}\frac{\dot{\beta}}{\Omega} \tag{11}$$

where $k_{\theta 1}$ is the pitch flap angle coupling coefficient and $k_{\theta 2}$ is the pitch flap rate coupling coefficient. ***

Figure 10 shows the impacts of pitch flap coupling terms on the blade pitch angle (assuming cyclic control is not applied). The pitch flap angle coupling is common for conventional helicopters. The flapping motion of the blade will slightly change the blade pitch angle if the pitch control rod is not located on the flapping axis. A positive $k_{\theta 1}$ indicates that the pitch angle will be increased when the flapping angle (β) is positive, as shown in Fig. 10.b. In the case of pitch flap rate coupling, the change in the pitch angle is associated with the blade flapping rate. A positive $k_{\theta 2}$ indicates that the pitch angle will be increased when the blade is flapping upwards ($\dot{\beta} > 0$), see Fig. 10.c.

Sensitivity analyses

The following design parameters will be investigated in the following sensitivity analyses: the rotor radius, blade area, rotor

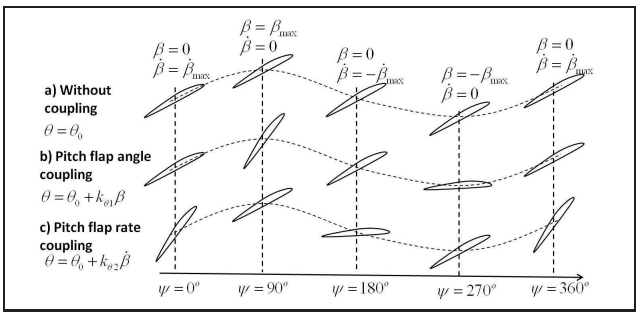

Figure 10: Sketch for blade pitch flap coupling

tip velocity, the fin size and the pitch-flap coupling.

The sensitivities of the required power and the stall area with respect to the above chosen design parameters will be investigated. Calculations will be performed for two flight conditions, including hovering and fast forward flight at 120 knots.

In the following figures, the required power is normalized by the maximum continuous engine power, and the stall area is normalized by the rotor disk area. All the design parameters are normalized by their values in the baseline design (Bo-105) respectively, except the pitch flapping coupling parameters (both $k_{\theta 1}$ and $k_{\theta 2}$) (their values in the baseline design are zero).

The rotor radius

The effects of changing the rotor radius on the Ornicopter's performance are shown in Fig. 11 with regard to the non-dimensional stall area $\bar{S}$ and the required power $\bar{P}$.

One can see the large improvements in the Ornicopter performance with the increase in the rotor radius in hovering. When a larger rotor is used, lower power is required and a smaller rotor area encounters stall (in percentage). In forward flight, the required power can also be reduced by using a larger rotor, while the stall area will be slightly increased.

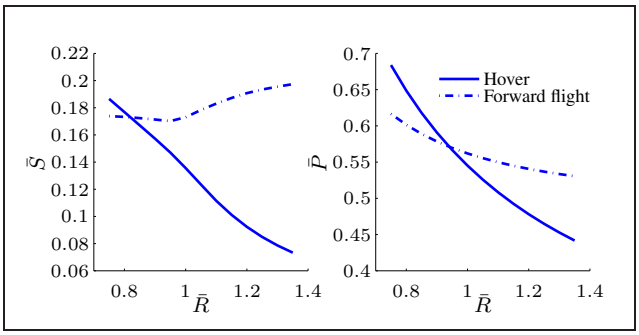

Figure 11: Impact of the rotor radius on the stall area and required power

By increasing the rotor radius, the induced velocity can by reduced, and hence lower induced power is required. As the induced power is the major part of the required power of helicopters in hovering, using a larger rotor can dramatically reduce the total required power of the Ornicopter. In forward flight, it is less beneficial to increase the rotor radius as the parasitic power is the dominant factor at high speed.

It has been proven that the amplitude of active flapping is associated with the forced flapping power [7]. By reducing the required power i.e. the forced flapping power, the amplitude of the active flapping can be reduced.

The simple Ornicopter rotor model in hovering (see Appendix A) can be used for more detailed analyses. In the trimmed hovering condition, the shaft torque coefficient should be zero. Equation. 33 can be rewritten as (cyclic pitch control is not considered):

$$0 = \frac{1}{2}\sigma_s C_{L_\alpha}\alpha_e\lambda_i + \frac{1}{8}\sigma_s C_{d0} - \frac{1}{16}\sigma_s C_{L_\alpha}\hat{\beta}^2 \tag{12}$$

in which the effective angle of attack α_e is :

$$\alpha_e = \frac{\theta_0}{3} - \frac{\lambda_i}{2} \tag{13}$$

The required flapping amplitude can be calculated as:

$$\hat{\beta}^2 = 8\alpha_e\lambda_i + 2\frac{C_{d0}}{C_{L_\alpha}} \tag{14}$$

Rewriting the main rotor thrust (see Eq. 29) gives:

$$\begin{aligned} T =& \frac{1}{6}\rho\left(N_b c R\right) C_{L_\alpha}\left(\Omega R\right)^2\theta_0 - \frac{1}{4}\rho\left(N_b c R\right) C_{L_\alpha}\left(\Omega R\right)^2\frac{v_i}{\Omega R} \\ =& \frac{1}{6}\rho A_b C_{L_\alpha} V_t^2\theta_0 - \frac{1}{4}\rho A_b C_{L_\alpha} V_t^2\frac{v_i}{V_t} \\ =& \frac{1}{2}\rho A_b V_t^2 C_{L_\alpha}\left(\frac{\theta_0}{3} - \frac{\lambda_i}{2}\right) \\ =& \frac{1}{2}\rho A_b V_t^2 C_{L_\alpha}\alpha_e \end{aligned} \tag{15}$$

In hovering, the thrust of the main rotor equals the total weight, which is assumed to be constant. Therefore, the α_e will keep constant as the blade area and tip velocity are constant while the rotor radius is varying. Meanwhile, the inflow ratio (λ_i) will decrease with the increase in the rotor radius. Combining these effects, one can find that increasing the rotor radius will decrease both the collective pitch (see Eq. 13) and the active flapping amplitude (see Eq. 14) in hovering, as shown in Fig. 12.

As discussed before, the reason why the Ornicopter's rotor encounters stall in hovering is that the active flapping introduces an additional variation of the blade angle of attack. By reducing the active flapping and collective pitch, both the mean angle of attack and the variation of the angle of attack can be reduced, and hence the stall area can also be reduced. Hereby, with regard to stall, the Ornicopter performance can be improved by increasing the rotor radius.

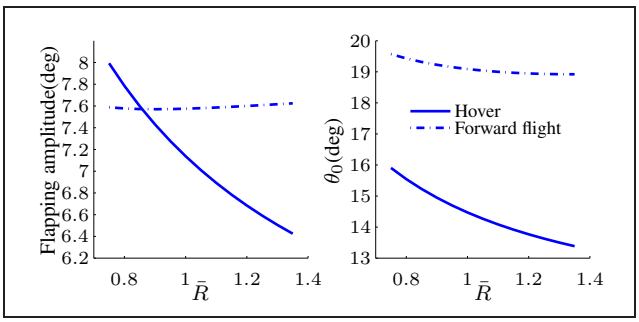

Figure 12: Flapping amplitude and collective pitch as a function of the rotor radius

In forward flight, the numerical calculations can show the effects of varying rotor radius on the active flapping and collective pitch control. Figure 12 shows that changing the rotor radius has less effect on the amplitude of active flapping and collective pitch control in forward flight than in hovering. As the induced power is a small part of the total required power in forward flight, the active flapping is almost constant while varying rotor radius. Due to the slightly reduced induced velocity, the collective pitch control also reduces slightly.

The increasing rotor radius also changes the flapping dynamics of the Ornicopter rotor. With a larger rotor, a higher negative longitudinal cyclic pitch control (θ_{s1}) is required for trimmed forward flight, which increases the blade pitch angle on the retreating side. This will increase the stall on the retreating blades. Therefore, the stall area will increase with an increase in the rotor radius in forward flight.

The blade area

Figure 13 shows the impact of the blade area on the Ornicopter performance. As the rotor radius is constant in this case, the rotor solidity will also change proportionally with the blade area.

The blade area is directly related to the blade loading ($M_a g/A_b$). By increasing the blade area, the blade loading will be smaller, and the local blade element angle of attack can be reduced for both hovering and forward flight. Recalling Eq. 15, the equivalent angle of attack (α_e) is inversely proportional to the blade area, i.e. it will decrease with an increase in the blade area. The blade area will not affect the induced velocity, i.e. the inflow ratio is constant. In this sense, the required collective pitch angle reduces in line with an increase in the blade area (see Eq. 13). From Eq. 14, one can see that the amplitude of the flapping motion also drops off for a lower equivalent blade angle of attack (α_e). The variation in the active flapping amplitude and collective pitch with the blade area is presented in Fig. 14. Due to the effects discussed above, increasing the blade area results in the stall area dropping off dramatically.

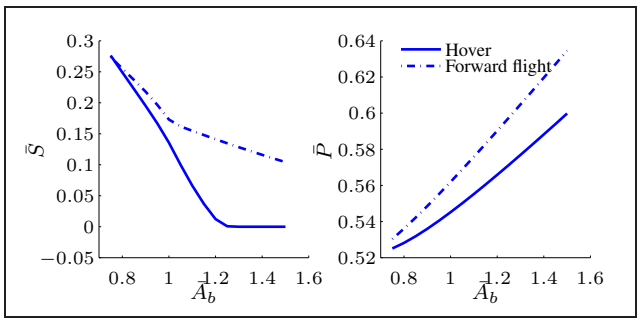

Figure 13: Impact of the blade area on the stall area and required power

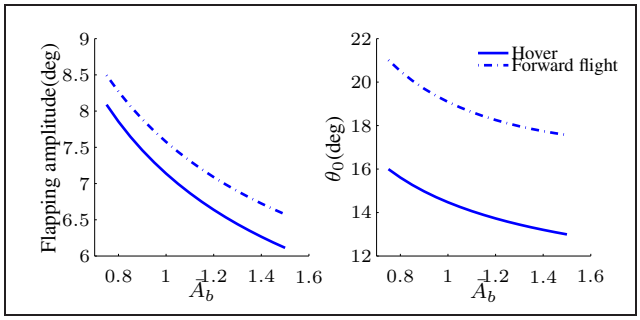

Figure 14: Impact of the blade area on the flapping amplitude and collective pitch

This is accompanied by higher power consumption due to the higher profile power, which is proportional to the blade area. In forward flight, more additional profile power is required because of higher local velocity on the blade element.

The tip velocity

In the case of tip velocity, its effect on performance is similar to that of the blade area. The higher the tip velocity is, the more dramatically the stall area drops and the required power increases, see Fig. 15.

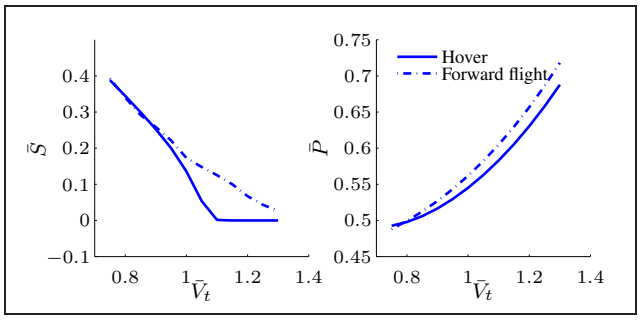

Figure 15: Impact of the tip velocity on the stall area and required power

The reduction of the stall area with increasing tip velocity is also caused by the lower flapping amplitude and collective pitch, similarly to the case of the blade area. However, varying the tip velocity has a greater effect on the Ornicopter's performance

than changing the blade area. This is due to the fact that aerodynamic forces are affected by the square of velocity (V_t^2). In hovering, using about a 10% higher tip velocity can eliminate the stall area, while it requires about a 20% larger blade area to obtain the same effect.

The fin size

The yaw moment generated by the vertical fin is negligible at low speed. In this sense, the vertical fin will only affect the performance of the Ornicopter in forward flight, as shown in Fig. 16 and 17.

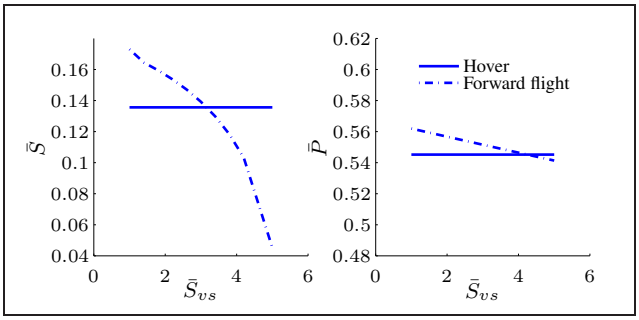

Figure 16: Impact of the fin size on the stall area and required power

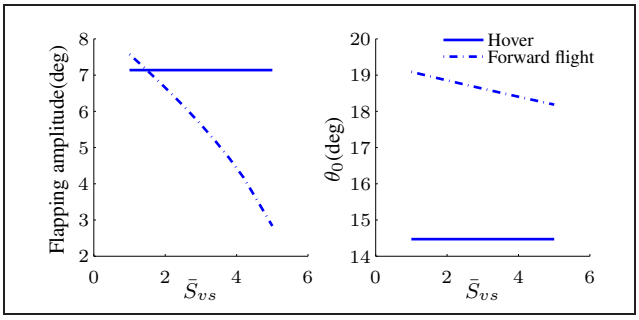

Figure 17: Impact of the fin size on the flapping amplitude and collective pitch

By using the vertical fin to compensate for a part of the shaft torque, less propulsive torque generated by the active flapping is required, and hence the amplitude of the forced flapping motion can be reduced, as shown in Fig. 17. In this way, the stall area in forward flight can be limited and the flight envelope of the Ornicopter can be extended. By reducing the active flapping, the rotor profile power can be reduced. As the profile power is not the main part of the total power in forward flight, a modest reduction in the required power can be found while increasing the fin size.

The pitch flap coupling

As shown in Eq. 11, two pitch flap couplings are considered in the flight mechanics model developed in this paper, including the pitch flap angle coupling ($k_{\theta 1}$) and the pitch flap rate coupling ($k_{\theta 2}$).

The pitch flap angle coupling. Figure 18 presents the impacts of the pitch flap angle coupling on the stall area and the required power of the Ornicopter. One can see that this coupling term has a relatively small effect on the stall area (it only varies by around 3%) and it will not noticeably affect the Ornicopter's required power either in hovering or forward flight.

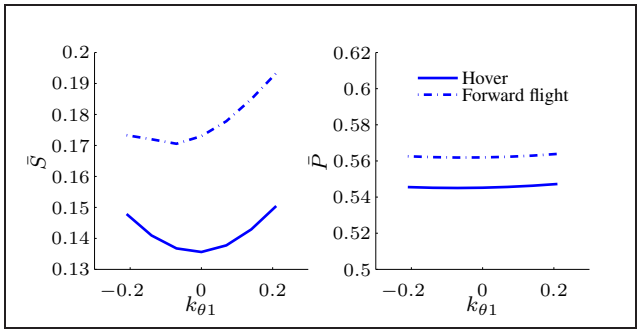

Figure 18: Impact of the pitch flap angle coupling on the stall area and required power

As mentioned above, the pitch flap angle coupling will change the blade pitch angle when the blade is not at the neutral position (in the flapping direction). This additional pitch angle will slightly enlarge the angle of attack variation amplitude on the blade elements. For example, considering a hovering Ornicopter rotor without cyclic control, the angle of attack of a blade element is: ***

$$\alpha = \theta - \varphi \tag{16}$$

where θ is the pitch angle of the blade and φ is the induced angle. Substituting Eq. 24 and 25 into Eq. 16, one can get: ***

$$\begin{aligned}\alpha =& \theta_0 + \theta_{tw}\bar{r} + \frac{\lambda_i}{\bar{r}} + k_{\theta 1}\beta_0 \\ &+ (k_{\theta 1}\beta_{s1} + \beta_{c1})\sin(\psi) + (k_{\theta 1}\beta_{c1} - \beta_{s1})\cos(\psi)\end{aligned} \tag{17}$$

The angle of attack variation amplitude is then:

$$\begin{aligned}\hat{\alpha} =& \sqrt{(k_{\theta 1}\beta_{s1} + \beta_{c1})^2 + (k_{\theta 1}\beta_{c1} - \beta_{s1})^2} \\ =& \sqrt{k_{\theta 1}^2 + 1}\sqrt{\beta_{s1}^2 + \beta_{c1}^2}\end{aligned} \tag{18}$$

From Eq. 18 one can see that the variation of the blade angle of attack will be enlarged by both the positive and negative values of the pitch flap angle coupling, assuming that the flapping motion is not affected by $k_{\theta 1}$. Calculations also show that this coupling term has no influence on the active flapping amplitude, as shown in Fig. 19. In this sense, when the $k_{\theta 1}$ is zero, the stall area has its minimum value, and increases for both positive and negative $k_{\theta 1}$.

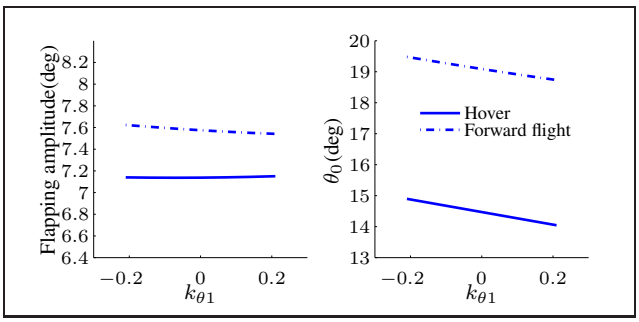

Figure 19: Impact of the pitch flap angle coupling on the flapping amplitude and collective pitch

In forward flight, similar impacts of $k_{\theta 1}$ as in hover can be found. However, due to the unsymmetrical airflow, positive and negative $k_{\theta 1}$ have slightly different impacts on the stall area. The stall area will reach its minimum value when $k_{\theta 1}$ is around -0.05.

The pitch flap rate coupling. While the blade is flapping downwards, the blade element angle of attack will be increased due to the flapping motion. This higher angle of attack will increase the stall area of the Ornicopter rotor. By using a positive pitch flap rate coupling, the blade angle of attack can be reduced as the pitch angle is reduced by the pitch flap rate coupling term.

In hovering, this effect can reduce the angle of attack variation on blade elements, as well as the maximum angle of attack. Therefore, the stall area can be reduced (see Fig. 20). Due to the lower local angle of attack, the average profile drag will also be lower. In this sense, the required power in hovering reduces slightly in line with the increasing $k_{\theta 2}$.

This coupling effect also reduces the propulsive force generated by the active flapping. During the down stroke, where the propulsive force is produced, the pitch angle is reduced by the pitch flap rate coupling, and hence less lift and propulsive fore are generated. On the other hand, the drag force increases in the upstroke due to the higher pitch angle. Therefore, the average propulsive force drops off, which requires the amplitude of active flapping to be increased, as shown in Fig. 21.

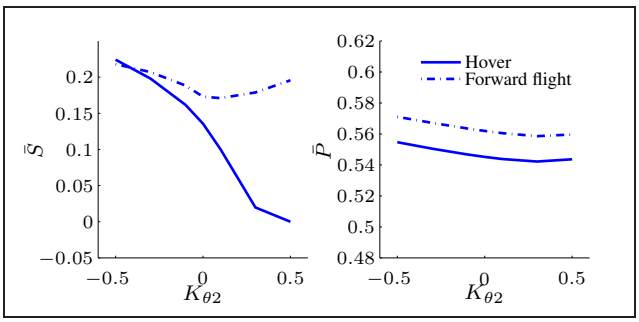

Figure 20: Impact of the pitch flap rate coupling on the stall area and required power

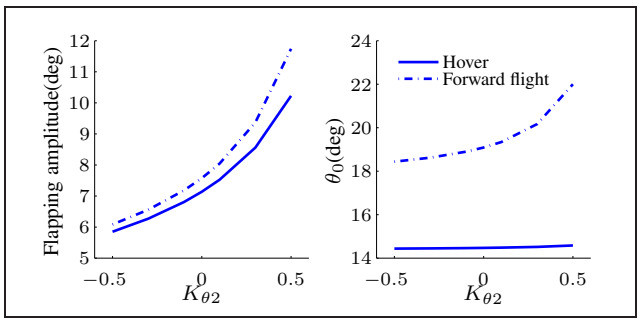

Figure 21: Impact of the pitch flap rate coupling on the flapping amplitude and collective pitch

It should be mentioned that though the amplitude of active flapping increases while higher $k_{\theta 2}$ is used, the local angle of attack on the blade element will increase more gradually. A higher flapping amplitude also indicates a higher flapping rate. As the change of pitch angle due to the pitch flapping rate coupling is proportional to the flapping rate, a higher flapping amplitude also means a larger reduction of pitch angle when the blade is flapping downwards ($k_{\theta 2} > 0$).

It can also be found that the collective pitch control will not be affected by this coupling effect in hovering, as shown in Fig. 21. In hovering, as there is no unsymmetrical incoming airflow, the average impact of the coupling on the rotor thrust in one revolution is zero. Hereby, the collective pitch control will be kept constant for different $k_{\theta 2}$ in hovering.

Overall, the total effect of a positive $k_{\theta 2}$ is a strong reduction of the stall area in hovering, as shown in Fig. 20.

For forward flight, the situation is different. The amplitude of active flapping will increase while increasing $k_{\theta 2}$, similar to in hovering. However, the collective pitch control will increase in this case. From Fig. 21, one can see that when negative $k_{\theta 2}$ is used, the collective pitch is increasing slowly with increasing $k_{\theta 2}$. Meanwhile, the gradient of the curve also increases, resulting in a rapidly increasing collective pitch when $k_{\theta 2}$ is close to 0.5.

Combining the two effects from above, the variation in the stall area in forward flight as a function of $k_{\theta 2}$ is characterized by a bucket shape. While $k_{\theta 2}$ is negative, the stall area can be reduced by increasing $k_{\theta 2}$, similar to in hovering. When $k_{\theta 2}$ is positive, increasing collective pitch becomes the dominant effect, and causes a higher stall area.

Design space

In the previous section, analyses were performed that varied only one design parameter at one time. Analyses for combina-

tions of multiple design parameters can show more information regarding the Ornicopter characteristics. In this sense, a database consisting of a large number of different Ornicopter designs is desired.

As mentioned above, four parameters were chosen for the design database, and their values are shown in Tab. 3. Most of the design combinations from Tab. 3 are included in the database, this resulting in more than 1×10^4 designs.

Table 3. Variation of the design parameters

Parameter	Initial design	Mini. value	Mini. %	Max. value	Max. %	Design points	Unit
R	4.91	3.68	75	6.63	135	13	m
A_b	5.30	3.98	75	7.95	150	16	m^2
V_t	218	164	75	283	130	12	m/s
S_{vs}	0.710	0.710	100	3.55	500	6	m^2

Using the design database, more analyses can be performed for the Ornicopter concept. One of the important applications is to find a feasible design space for certain design requirements. In this section, the feasible design space for the Ornicopter based on the Bo-105 performance shown in Tab. 2 will be investigated.

Defining the design criteria

The design requirements are defined based on the performance specification in Tab. 2, i.e. the hovering ceiling and maximum velocity. They can be converted into the required power and stall area limitations in certain flight conditions to reduce the calculation cost.

For example, to predict the maximum speed of a helicopter limited by the stall area, numerical methods will be used to search for the velocity at which the rotor stall area reaches the maximum value allowed. This means that analyses need to be performed for several velocities. The stall area increases with increasing flight velocity. Therefore, if the stall area of one design does not reach the maximum stall allowed at the maximum speed requirement (V_{max}^{req}), it can fly faster than V_{max}^{req}, i.e. it satisfies the design requirement. In this way, the stall analysis only needs to be performed once, and the computation cost can be reduced dramatically.

To get more understanding of the influences of different designs on the Ornicopter performance, the sea level hovering condition is also considered in this section. In this sense, three flight conditions are chosen for the analyses: hovering at sea level (referred to as hovering in the following), maximum speed forward flight (150 knots) at sea level, and hovering ceiling (2815 m).

The required power and stall area will be analyzed for each condition and the analysis results for the Bo-105 helicopter will be used as design requirements for the Ornicopter design. In other words, the Ornicopter design should have the same or lower power consumption and stall area than the Bo-105 helicopter.

It should be noticed that the Bo-105 rotor does not encounter stall in hovering, while the Ornicopter concept introduces stall in hovering due to active flapping. The same stall area requirement will be applied to the Ornicopter in hovering conditions (both sea level and hovering ceiling) as for forward flight.

All the design requirements with regard to stall and power (in non-dimensional form) are summarized in Table. 4.

Table 4. Design requirements

Flight condition	Velocity	0	0	150 knots
	Altitude	0	2815 m	0
Maximum stall		0.0893	0.0893	0.0893
Maximum power		0.543	0.584	0.846

Results from the design database

Based on these design requirements discussed above, a feasible design space for the Ornicopter can be determined. As the four design parameters vary, the feasible design space will be a four-dimensional space, which is difficult to visualize. To have a better view of the design space and the impacts of varying parameters on it, the feasible rotor sizing (i.e. rotor radius and blade area) is presented for different tip velocities and vertical fin size. Besides the stall and power requirements mentioned above, the allowable blade aspect ratio (R/c) is also limited, for example by the blade structure design. In the following figures, the aspect ratio limitation is also presented ($14 < R/c < 20$).

Figure 22 shows the feasible rotor design boundary for different tip velocities based on the sea level hovering requirements.

For the stall requirement, the feasible design space is on the top-right side of the boundary, due to the fact that a higher rotor radius and blade area can reduce the stall area. In the case of the required power, a higher rotor radius and lower blade area will be beneficial. Therefore, the feasible design space is on the bottom-right side of the boundary.

Increasing the tip velocity, both the boundaries for stall and power will shift. As increasing the tip velocity dramatically reduces the stall area, a lower blade area and rotor radius are required to keep the stall area lower than the design requirement. The stall boundary moves towards the bottom-left side

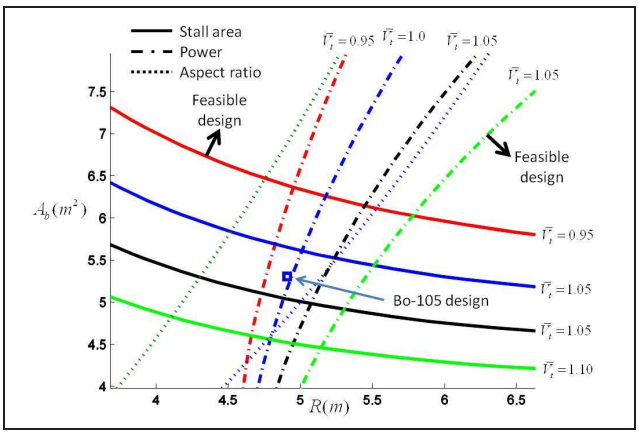

Figure 22: Design space with different tip velocities for hovering ($\bar{S}_{vs} = 5$)

and the feasible design area for stall requirement is enlarged. Meanwhile, the higher the tip velocity is, the larger the profile power required. To maintain the same total power consumption, a higher rotor radius should be used to reduce the induced power or the blade area should be lower to reduce the profile power. This effect moves the power boundary towards the right-hand side and reduces the feasible design space.

The design boundaries change with the variation in the tip velocity. For all the tip velocities presented in Fig. 22, a design space can be found that fulfills both the stall and power requirements. This feasible design space moves from the top-right corner to bottom-right when the tip velocity is increasing.

Similar results can be found for the hovering ceiling requirement, as shown in Fig. 23. Two major differences can be found when comparing this to the sea level hovering condition.

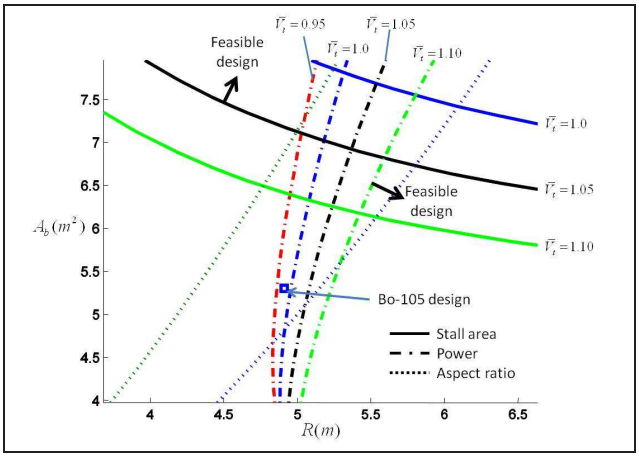

Figure 23: Design space with different tip velocities for the hovering ceiling condition ($\bar{S}_{vs} = 5$)

First, the stall boundary shifts to the top-right corner of the plot. This is caused by a higher stall area with an increased altitude. At high altitude, the air density becomes lower. To generate the same thrust, the rotor needs to accelerate more air (in volume), in other words, the induced velocity and inflow ratio will be higher. Meanwhile, the thinner air will also increase the required equivalent blade angle of attack, see Eq. 15. Recalling Eq. 14, the increasing α_e and inflow ratio will require a higher amplitude of active flapping for the same thrust. Combining these effects, the stall area of the Ornicopter rotor will increase with increasing altitude. Because of the higher stall area, a higher blade area and rotor radius are needed to match the stall design requirement, and hence the stall boundary moves.

Secondly, the power boundary slightly rotates and is more close to a vertical line when compared with the sea level hovering condition. The impact of tip velocity on the power constraint becomes smaller. This is caused by the fact that with increasing altitude, the profile power becomes a smaller part of the total required power. As the tip velocity only affects the profile power, it has less impact on the power constraint. Similarly, the blade area also has a small effect on the total required power. The rotor radius is the dominant factor for power requirement in this flight condition.

In fast forward flight, the design boundaries are different from hovering, as shown in Fig. 24

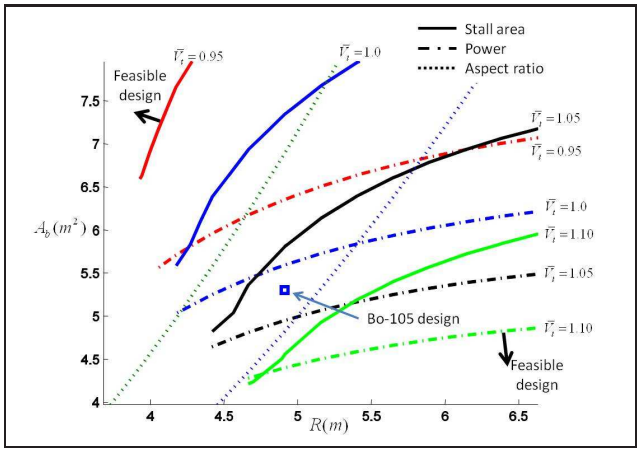

Figure 24: Design space with different tip velocities for forward flight ($\bar{S}_{vs} = 5$)

For the power requirement, the feasible design space is still on the bottom-right side of the boundary, which indicates that a smaller blade area and smaller rotor radius are preferable with regard to power consumption. In forward flight, the parasite power is the main part of the required power and it is determined by the fuselage design. The profile power is secondary and the induced power is the smallest proportion of the total required power. In this sense, the power boundary is relatively flat, i.e., the required power is more sensitive to the blade area than to the rotor radius.

Some major changes can be found on the stall boundaries. In the forward flight condition, the feasible design space is located on the top-left side of the stall boundary instead of the top-right side, which indicates the trend to use a smaller rotor. This can

also be found from the sensitivity analysis, as Fig. 11 shows a slightly increase in the stall area with an increase in rotor radius in forward flight.

One may have noticed that there is no intersection between the feasible design spaces defined by stall and power requirement respectively. This demonstrates that no feasible design space can be found for the Ornicopter in forward flight. While the tip velocity is increasing, both stall and power boundaries are shifting to the bottom-right side of the graph. The feasible design cannot be achieved by changing rotor tip velocity.

As discussed in the previous section, the Ornicopter active flapping blade will increase the stall area and the profile power of the main rotor. To reduce the stall area, a larger blade area or higher tip velocity should be used. However, those solutions will further increase the rotor profile power. In hovering, while the induced power is the major part of the total required power, by using a larger rotor radius, the required power can be reduced. At a certain point, the reduction in induced power can overcome the increasing of the profile power necessary for the stall requirement, resulting in a feasible Ornicopter design. In forward flight, the impact of the rotor radius on the required power is very small. Therefore, the power and stall requirements cannot be satisfied at the same time.

So far, the impacts of vertical fin size on the feasible design space have not been discussed. As the vertical fin does not generate any force or moment in hovering, it will not affect the Ornicopter performance in hovering. In this sense, only the design boundaries in the forward flight condition will be shown, see Fig. 25.

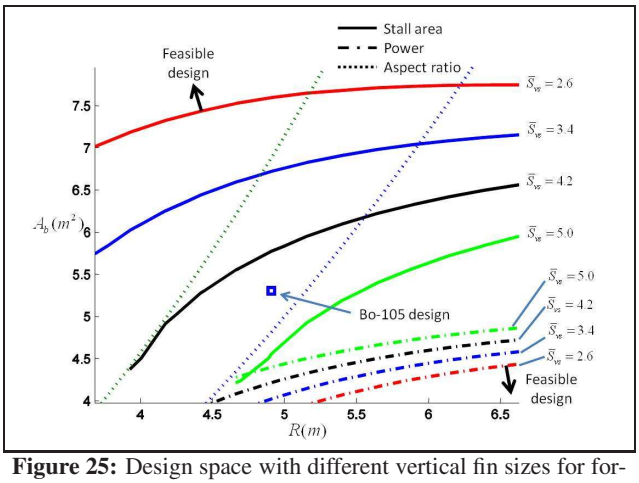

Figure 25: Design space with different vertical fin sizes for forward flight ($\bar{V}_t = 1.1$)

The general shape of the stall boundaries is similar to those boundaries drawn while changing tip velocity. By increasing the fin size, the Ornicopter's feasible design space can be greatly enlarged.

For the power boundary, the vertical fin size is less influential. However, increasing the vertical fin size is beneficial for the power boundary. Though a feasible design space cannot be found for the fin designs shown in Fig. 25, the stall and power boundaries are moving towards each other. At a certain point, when the vertical fin is large enough, a feasible design will be found. This will happen when the vertical fin compensates for all the main rotor shaft torque. The active flapping will not be needed. In this case, the Ornicopter rotor will work as a conventional helicopter rotor. The stall area and required power should be very close to those of a conventional helicopter. Meanwhile, the tail rotor does not exist on the Ornicopter. The Ornicopter total required power can be smaller than that of the Bo-105 helicopter. This results in a feasible design space for the Ornicopter in the forward flight condition. ***

However, this will require a large equivalent fin area (S_e), which will cause other drawbacks. One of them is a lack of yaw control. If the vertical fin compensates for all the shaft torque and the amplitude of the active flapping is zero, the Ornicopter rotor will work as a conventional helicopter rotor, and hence it will not be able to generate a yaw control moment in both directions. An additional yaw control method is needed, such as the use of a rudder. Meanwhile, a large vertical fin may also cause some problems regarding the structure or weight. More research should be carried out for a proper fin design in future work.

Compromised design requirements

As shown above, a design space for the Ornicopter that fulfills the requirements for all three flight conditions cannot be found. The most critical condition is at the maximum forward flight velocity. This indicates that the final Ornicopter design will have a higher power consumption and/or smaller flight envelope.

In this sense, the design requirements should be modified. Some requirements have to be compromised to achieve a satisfactory design.

For the power requirement, the allowed power consumption can be increased for each flight condition. This results in an Ornicopter design that has higher required power than the Bo-105 helicopter. Figure 26 shows all the design boundaries in all three flight conditions. The maximum power consumption in this case is increased by 10%. A feasible design space can now be found.

It can be found that the feasible Ornicopter design will have a higher blade area and tip velocity to reduce the stall area. This will also increase the profile power of the rotor. Therefore, the

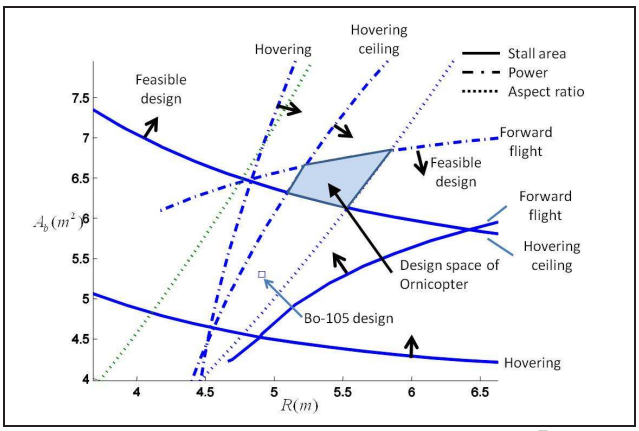

Figure 26: Feasible design space (10% higher power, $\bar{V}_t = 1.1$, $\bar{S}_{vs} = 5.0$)

rotor radius will also be increased to reduce the induced power. However, reducing the induced power cannot compensate for all the additional profile power, resulting in a higher total required power for the Ornicopter.

In the case of the stall requirements, a similar calculation as for the power requirement is performed, as shown in Fig. 27. In this case the stall area limitations are increased by 20%.

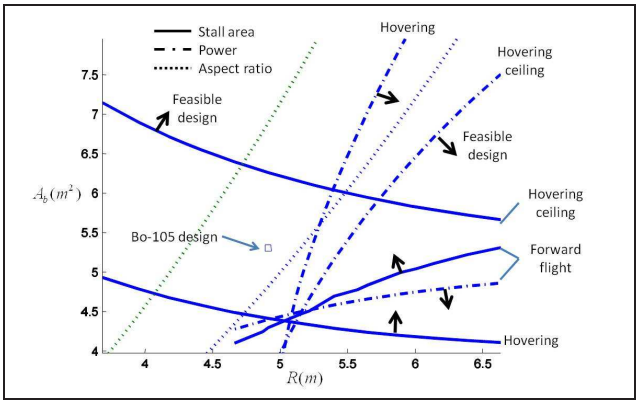

Figure 27: Feasible design space (20% larger stall area, $\bar{V}_t = 1.1$, $\bar{S}_{vs} = 5$)

From Fig. 27 one can see that with the higher allowable stall area, the design boundaries for the stall requirements shift only slightly. Hence, no feasible design space can be found in this case.

Comparing Fig. 26 and 27, it can be found that the design boundaries of the power requirements are significantly more sensitive to the design requirements than the stall boundaries.

This is caused by the fact that these design parameters have higher impacts on the stall area than on the required power. For example, recalling the sensitivity analyses shown in Fig. 13, the stall area varies by about 100% of the initial value in forward flight, while the variation in required power is only about 20%.

In this sense, while changing the stall design requirements, the stall design boundaries only move slightly. Therefore, no feasible design space can be found when increasing the allowed stall area by 20%.

In order to obtain a feasible design, the stall requirements need to be further relaxed, which means a very small flight envelope. In this way, the required power of the Ornicopter can be kept the same as the Bo-105. However, the small flight envelope will be a major drawback for this design.

In conclusion, from the above analyses, it appears that the power requirements should be relaxed to enable a feasible Ornicopter design, and the stall requirements can be kept the same as proposed before. The resulting Ornicopter design will have a similar flight envelope as the Bo-105 helicopter but a higher power consumption.

Design optimization

Defining cost function and constraints

From the analyses of the design space, it was concluded that to maintain the same required power as the Bo-105 helicopter, the Ornicopter has to compromise its flight envelope. It will be a better option to design an Ornicopter with a similar flight envelope to the Bo-105, while requiring slightly more power. Therefore, the stall requirement will be considered as design constraints and the required power will be used as the optimization objective.

As discussed before, the stall area on the Ornicopter rotor in hovering will increase with increasing altitude. Therefore, for a certain design, the stall area in the hovering ceiling condition will always be larger than that of sea level hovering. The maximum allowed stall areas are the same for all flight conditions. Therefore, a design will be satisfactory with regard to the stall requirement at sea level if it satisfies the stall requirement at high altitude. It is not necessary to include the stall requirement in hovering at sea level as design constraints of the optimization.

In this sense, the main constraints of the design include the stall area at the hovering ceiling and in forward flight (150 knots), as well as the blade aspect ratio limitation, as:

$$\begin{cases} \bar{S}_{hc} < 0.0893 \\ \bar{S}_f < 0.0893 \\ 14 \leq R/c \leq 20 \end{cases} \tag{19}$$

The optimization objective is the Ornicopter's required power in the three flight conditions used before. As there are multiple flight conditions, the results should be combined to form one scalar objective function. The following weight fac-

tor is used for this purpose:

$$F = w_f \bar{P}_f + \frac{1 - w_f}{2} \left(\bar{P}_h + \bar{P}_{hc} \right) \tag{20}$$

where w_f is the weight factor for required power in forward flight, $\bar{P}_f$, $\bar{P}_h$ and $\bar{P}_{hc}$ are the normalized required power in three flight conditions (forward flight, sea level hovering and hovering ceiling respectively), which represent the ratio of the required power of the Ornicopter to that of the Bo-105 helicopter, as:

$$\begin{aligned} \bar{P}_f &\equiv \frac{P_f^{(Orni)}}{P_f^{(Bo)}} \\ \bar{P}_h &\equiv \frac{P_h^{(Orni)}}{P_h^{(Bo)}} \\ \bar{P}_{hc} &\equiv \frac{P_{hc}^{(Orni)}}{P_{hc}^{(Bo)}} \end{aligned} \tag{21}$$

By tuning the weight factor, optimal designs can be obtained for different flight conditions. The value of the weight factor will depend on the desired Ornicopter applications. For example, the Ornicopter designed for troop transportation will mainly fly at high velocity, and hence a large w_f should be considered ($0.5 < w_f < 1.0$). To investigate the impacts of the weight factor on the final Ornicopter design, different values are tested. The optimization results will be presented in the following section.

The optimization tool provided by $Matlab$ ($fmincon$) is used for the design optimization. This can find the minimum value of the constrained non-linear multi-variable function. The interior point algorithm provided by $fmincon$ is used for the following optimization. It will not be further discussed in detail as it is a standard method. More details of the algorithm were discussed in Ref [19, 20].

The design optimizations are performed with different weight factors w_f, ranging from 0 to 1.0. In this sense, a series of optimal designs are obtained.

Optimization results

Before presenting all the optimization results, the optimization history data for one case ($w_f = 0.5$) is presented. Figure. 28 shows the history of design parameters with their upper (UL) and lower limits (LL). In Fig. 29, the design constraints (blade aspect ratio and rotor stall area) are presented.

The optimization starts with the Bo-105 design. It is not satisfactory due to the high stall area. The optimization algorithm first searches for a feasible design, resulting in a very high tip velocity. From this design, the search direction follows the trend of using a larger rotor radius and blade area, lower tip velocity and a small negative $k_{\theta 2}$.

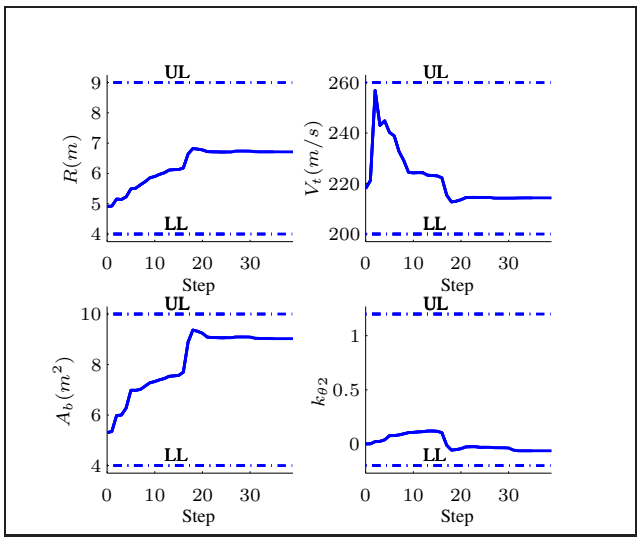

Figure 28: Design parameter history for $w_f = 0.5$

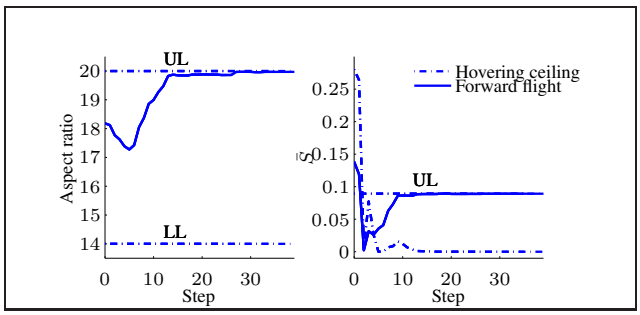

Figure 29: Design constraints for $w_f = 0.5$

From Fig. 28 and 29, one can see that the design parameters do not reach the limitations, and the active constraints for this optimization case are the blade aspect ratio and stall area in forward flight.

To understand the trend of the optimized Ornicopter design and the active constraints, all the optimization results ($0.0 \leqslant w_f \leqslant 1.0$) are analyzed together. The physical reasons causing these results will be investigated.

Figure 30 presents the normalized power requirement of the optimal Ornicopter designs with different w_f. It clearly shows that the required power in the hovering condition and forward flight are contradictory.

With a low weight factor, the Ornicopter design can be optimized mainly for hovering, resulting in approximately 7% less required power in hovering and 15% power requirement reduction at the hovering ceiling, when compared to the Bo-105. The drawback that comes with this design is the higher required power in forward flight, which is about 11% higher than that of the Bo-105 helicopter.

Similar results can be found for the high w_f cases, in which the forward flight performance is the main optimization objective. However, the optimal Ornicopter design will still have higher required power than the Bo-105 in forward flight (ap-

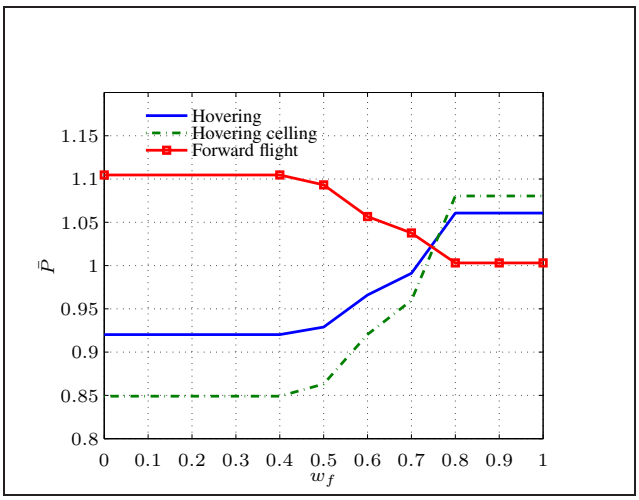

Figure 30: Normalised required power of the optimal Ornicopter design as a function of w_f

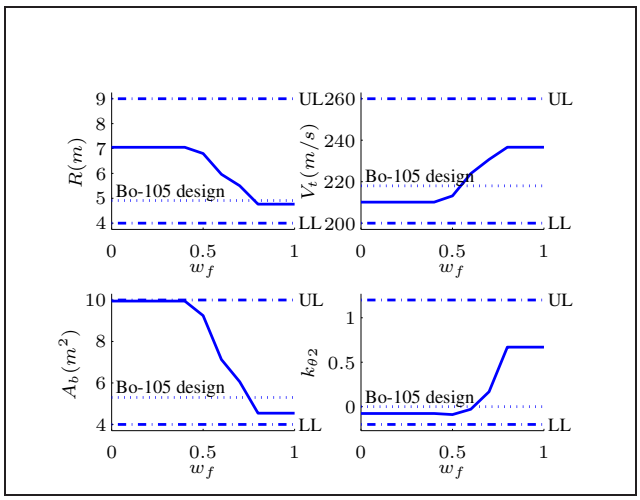

Figure 31: Optimal designs for different w_f

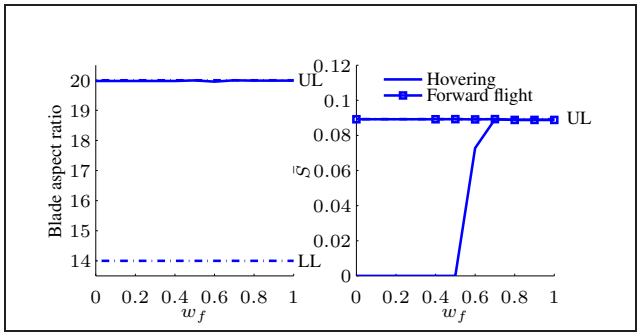

Figure 32: Design requirements at different w_f

proximately 1%), and the required power in hovering will be increased dramatically (close to 8%). In other words, to reduce the Ornicopter power consumption in forward flight, the hovering performance needs to be compromised to a large extent.

From Fig. 30, one can also find that the impact of w_f on the hovering performance is much higher than in the forward flight condition. The change of normalized power requirement at the hovering ceiling is nearly 25%, while the required power in forward flight varies by only around 10%.

This is caused by the fact that the induced power is the dominant part in the total required power in hovering, and it is very sensitive to the design parameters considered in the above optimization, especially the rotor radius. In forward flight, the fuselage parasitic power is the main part of the total required power, which is not affected by the rotor design parameters.

Figure 30 also shows that the optimal design is not affected for low and high weight factors, i.e. the w_f is influential mainly in the range of 0.4 to 0.8. For a better understanding of Ornicopter's the optimization results, the variations in the optimal design parameters (as a function of w_f) are presented in Fig. 31, and Fig. 32 shows the blade aspect ratio and rotor stall area of the optimal designs.

From Fig. 31 and 32, one can see that the optimal design reaches the boundary (boundary for design parameters or stall boundary) when w_f is lower than 0.4 or higher than 0.8.

When w_f is low, the design is optimized mainly for hovering, where a higher rotor radius is desired to reduce the induced power. Due to the design constraint of the maximum blade aspect ratio, the blade chord length also needs to be increased. At the point where w_f is 0.4, the blade area reaches the maximum value allowed. In this sense, the required power in hovering cannot be further reduced when lowering w_f.

Increasing w_f (between 0.4 and 0.8), the required power for forward flight becomes a larger part of the optimization objective. To reduce the forward flight power consumption, the blade area needs to be reduced, in order to minimize the profile power. Due to the blade aspect ratio constraint, the rotor radius should also be reduced. This will increase the induced power consumption. However, the induced power is very small in forward flight, and thus the total required power can be reduced by using a smaller rotor. Meanwhile, as shown before, a lower blade area also means a higher stall area. Therefore, the rotor tip velocity should be increased to delay the stall.

For the low w_f cases, due to the high blade area and rotor radius, the stall will not occur in the hovering ceiling condition (see Fig. 32). Increasing w_f, the optimal rotor radius and blade area decrease. This causes more stall in hovering. Therefore, the optimal pitch-flapping coupling will also increase, as this can reduce the stall area in hovering (see Fig. 20).

After w_f reaches 0.8, its effect on the optimal Ornicopter design becomes very small. This is due to the fact that the stall area reaches the design requirements in both hovering and forward flight conditions. In this situation, any design variation which can reduce the forward flight power consumption, such

as a smaller rotor or a lower tip velocity, will increase the stall area and results in an unsatisfactory design.

Overall, the weighing factor w_f will affect the final optimal Ornicopter design, and this plays an important role between the range of 0.4 and 0.8. The higher w_f is, the better the forward flight performance, which requires a smaller rotor size and blade area, as well as a higher tip velocity and pitch flapping rate coupling to reduce the stall area.

The final optimal Ornicopter design will depend on the potential applications of the helicopter. In this sense, it is not the intention of this paper to determine the 'best' Ornicopter design.

In this paper, the purpose of the Ornicopter design process is to find a design that has a similar performance to the reference helicopter Bo-105 and to investigate the potential of this new concept. Therefore, the optimization results which have similar required power to the Bo-105 for both hovering and forward flight should be considered as the Ornicopter design candidates.

Recalling Fig. 30, this shows that the Ornicopter concept is not a good solution for fast forward flight. Its minimum required power in forward flight is still higher than the power consumption of the Bo-105, while the cost to reduce it is very high (i.e. the required power in hovering increases dramatically). Meanwhile, to reduce the stall area, the rotor tip velocity should be increased, see Fig. 31. This will also degrade the Ornicopter high speed performance due to compressibility effects on the advancing side.

Overall, the optimal Ornicopter design corresponding to $w_f = 0.7$ has been chosen. The design parameters are presented in Tab. 5. The Ornicopter design has almost identical required power in hovering as the Bo-105 ($\bar{P}_h = 0.9911$) and lower required power at the hovering ceiling ($\bar{P}_{hc} = 0.9598$). As discussed before, the required power of the Ornicopter will be higher than that of the Bo-105. For the chosen Ornicopter design, it requires about 4% more power at 150 knots forward flight ($\bar{P}_f = 1.038$).

Table 5. Optimized Ornicopter rotor design

	Design parameters					
	R	A_b	V_t	$k_{\theta 2}$	c	Ω
	m	m^2	m/s		m	rad/s
Ornicopter	5.50	6.06	230.7	0.168	0.275	41.9
Bo-105	4.91	5.30	218.0	0	0.270	44.4

It should be mentioned that the vertical fin size used in the optimization is relatively high ($\bar{S}_{vs}$), in order to increase the equivalent vertical fin size (S_e). To limit the vertical fin size to a practical value, while keeping the same equivalent vertical fin size, the vertical fin size and the incidence angle are both increased for the following comparisons. The incidence angle (β_0^{fin}) is increased to 8° ($\bar{\beta}_0^{fin} = 1.72$) and the $\bar{S}_{vs}$ equals 2.91.

Comparisons with the Bo-105

In this section, the new optimized Ornicopter design will be compared with the Bo-105 helicopter. The comparisons will be done for the flight envelope, the natural modes and handling qualities.

The flight envelope of the new Ornicopter design as compared with the Bo-105 is presented in Fig. 33.

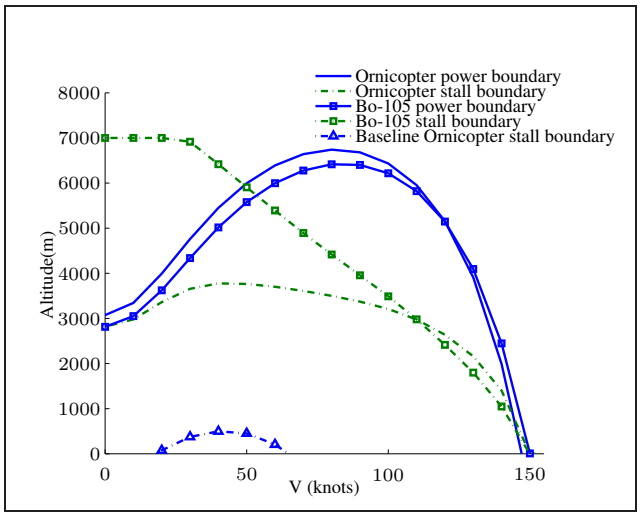

Figure 33: The flight envelope of the optimal Ornicopter and Bo-105

It can be found that the Ornicopter stall boundary is greatly extended when compared to the baseline design. For this new Ornicopter design, the flight envelope will be similar to that of the Bo-105 helicopter.

Looking at the stall boundary, one can see that the stall effect still has a large impact on the Ornicopter hovering performance when compared with the Bo-105. However, this optimized Ornicopter has dramatically increased the hovering ceiling defined by the stall effect.

Increasing the air speed, the stall service altitude of the Ornicopter will increase first until it reaches the maximum altitude at around 50 knots flight speed. Afterwards, it will decrease with the increase in speed. In the Bo-105 case, the stall service altitude will keep decreasing as the velocity increases.

This is caused by the fact that the stall area on the Ornicopter rotor consists of two parts: 1) the 'conventional' stall area caused by the blades' longitudinal flapping, the longitudinal cyclic control and the unsymmetrical local air flow, and 2) the stall intro-

duced by the active flapping.

As the amplitude of the active flapping is associated with the required power, it has a similar bucket shape as the required power for helicopters. This indicates that the stall caused by the active flapping will also have a bucket shape, which makes the stall boundary of the Ornicopter have a 'reversed' bucket shape as seen in Fig. 33.

One can also see that at high forward speed (around 130 knots), the Ornicopter has a higher stall service altitude than the Bo-105 helicopter. This shows that, in forward flight, the stall area on the Ornicopter rotor is less sensitive to altitude compared with a conventional helicopter main rotor.

For the same flight speed, increasing the altitude will increase the 'conventional' stall area on both the Ornicopter rotor and conventional helicopter rotor. For the Ornicopter, the stall area caused by the active flapping is associated with the required power. In fast forward flight, increasing the altitude decreases the air density, and hence the power required by the Ornicopter reduces (as the parasite power is the major part of the total required power). In this sense, the amplitude of active flapping will decrease as the altitude increases, as well as the stall area. Combining these two effects, the development of the stall area on the Ornicopter rotor is more gradual than that of the Bo-105 while the altitude is increasing. Therefore, in forward flight, the Ornicopter has a slightly higher service altitude than that of the Bo-105.

In hovering, the situation is reversed. Now the induced power is the main part of the required power. Increasing the induced power at higher altitude requires an increase in the amplitude of active flapping which causes a larger stall area. In this sense, the Ornicopter rotor stall area in hovering will increase very fast when the altitude is increasing resulting in much lower stall hovering ceiling than the Bo-105.

For the power boundaries, the Ornicopter shows a similar trend to conventional helicopters. At low and modest speed, the Ornicopter has a slightly higher service altitude than the Bo-105, while its maximum speed which is limited by the available power is lower.

This is also caused by the different compositions of required power in hovering and forward flight. Due to the stall effect, the Ornicopter needs a rotor with a higher radius, blade area and tip velocity. This design modification will reduce the induced power, while increasing the profile power. In this sense, compared with the Bo-105, the Ornicopter has lower required power in hovering, when induced power is the dominant part of the total required power, and higher required power in forward flight, when the profile power is higher than the induced power.

Combining stall and power boundaries, one can see that the Ornicopter will have a slightly better performance in hovering and low speed. Due to the higher stall area, the Ornicopter has a lower service ceiling when compared to the Bo-105. For high speed flight, the Ornicopter performance is worse than the Bo-105 due to the higher required power.

Conclusions

In this paper, some design parameters of the Ornicopter are modified based on its characteristics. The new optimized Ornicopter design is determined.

Sensitivity analyses are performed first to investigate the impacts of different design parameters on the Ornicopter performance. Based on the analyses results, four parameters are chosen to build a design database, including: the rotor radius, the blade area, the tip velocity and the vertical fin size.

Combining the different values of these four parameters, a design database is formed. From the database, it can be found that no feasible design can be found for the Ornicopter to satisfy both the design requirements, i.e. the stall area requirements and the required power requirements.

Using the optimization method, the optimal Ornicopter designs concerning different flight conditions (hovering or forward flight) are identified. The results show that the hovering performance of Ornicopter can be better than that of the Bo-105, with the cost of poorer forward flight performance. However, the optimal forward flight performance of the Ornicopter is always inferior to that of the Bo-105 due to the active flapping. This indicates that the Ornicopter concept might be more suitable for low and mid-range velocity applications.

From the series of optimal Ornicopter designs, the one with similar hovering performance to the Bo-105 is chosen as an example design, and compared with the Bo-105 in means of the flight envelope and handling qualities.

Comparisons show that the new Ornicopter design can greatly improve the limited flight envelope of the baseline Ornicopter design. The new design has a better altitude performance at low speed and fast forward flight, while having lower maximum speed due to the higher required power.

Future work

Several aspects of the Ornicopter's design process will be extended in the future. One of the future work relates to the total

weight of the Ornicopter. In the paper this weight is assumed to be constant. The weight of additional forced flapping mechanics should be estimated, as well as the weight reduction caused by the absence of the tail rotor. Meanwhile, the impacts of design parameters, such as a larger rotor and vertical fin, on the weight of the Ornicopter should also be considered.

Likewise, goals for Ornicopter's load alleviation need to be postulated. Technologies such as the HHC (high harmonic control), IBC (individual blade control) and variable RPM rotor, may also improve the Ornicopter concept, and should be considered in future research.

Finally, one of the critical issues for the Ornicopter is, as in the case of any helicopters, related to safety. Eliminating the tail rotor results in the increasing reliability of a helicopter. However, the Ornicopter concept introduces additional complexities on the main rotor. The effect of this revolutionary rotor concept on the helicopter's reliability requires a more detailed rotor hub design and should be considered in further analyses.In particular, the Ornicopter's behaviour after the failure of the forced flapping mechanism should also be investigated in future works.

Appendix: Ornicopter rotor model in hovering

In this appendix, a simple rotor model for the Ornicopter in hovering will be derived using blade element theory. A central hinged rotor is considered in this model, as shown in Fig. 34.

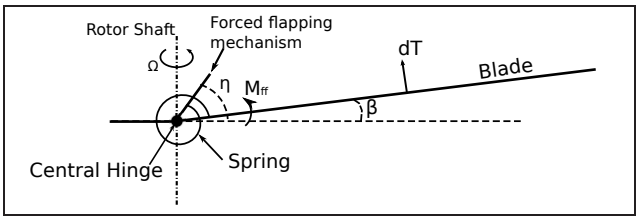

Figure 34: Blade configuration for the rotor model

The blade flap motion can be expressed as:

$$\beta = \beta_0 + \beta_{s1}\sin(\psi) + \beta_{c1}\sin(\psi) \tag{22}$$

The lift and drag forces on the blade element shown in Fig. 35 are:

$$\begin{aligned} dL &\approx \frac{1}{2}\rho v_t^2 C_{L_\alpha}(\theta - \varphi)cdr \\ dD &\approx \frac{1}{2}\rho v_t^2 C_{d0}cdr \end{aligned} \tag{23}$$

in which θ is the pitch angle of the blade defined as:

$$\theta = \theta_0 + \theta_{s1}\sin\psi + \theta_{c1}\cos\psi \tag{24}$$

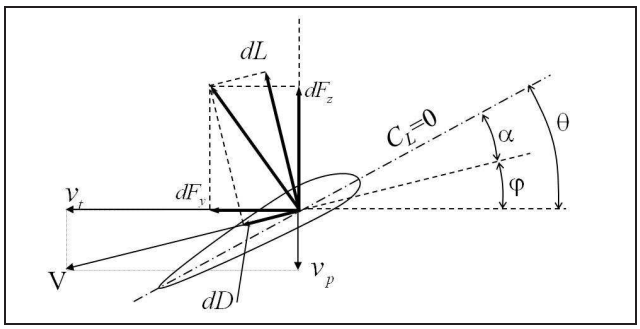

Figure 35: Aerodynamic environment at a typical blade element

and φ is the induced angle caused by the induced velocity and the blade flapping motion: ***

$$\varphi \approx \frac{\dot{\beta}r + v_i}{v_t} \tag{25}$$

The lift and drag forces can be expanded as;

$$\begin{aligned} dL &= \frac{1}{2}\rho C_{L_\alpha} c\left(\theta\Omega^2 r^2 - \Omega r\left(\dot{\beta}r + v_i\right)\right)dr \\ dD &= \frac{1}{2}\rho\Omega^2 r^2 C_{d0}cdr \end{aligned} \tag{26}$$

Assuming that the induced angle is small, one can obtain:

$$\begin{aligned} dF_y &\approx dD + dL\varphi \\ dF_z &\approx -dL \end{aligned} \tag{27}$$

Similarly, these forces can be transformed into the rotor shaft reference, thus in order to calculate the thrust and shaft torque generated by the rotor:

$$\begin{aligned} dT &\approx dL \\ dQ &\approx dF_y r \end{aligned} \tag{28}$$

where T is the rotor thrust and Q is the shaft torque.

Integrating through the blade radius and rotor azimuth angle gives the total hub forces and torque generated by one blade. The blade thrust is then:

$$T_s = \frac{1}{6}\rho c C_{L_\alpha}\Omega^2 R^3\theta_0 - \frac{1}{4}\rho c C_{L_\alpha}\Omega R^2 v_i \tag{29}$$ ***

It can also be written in non-dimensional form as:

$$\begin{aligned} C_{T_s} &= \frac{T_s}{\rho\left(\Omega R\right)^2\pi R^2} \\ &= \frac{1}{2}\sigma_s C_{L_\alpha}\left(\frac{\theta_0}{3} - \frac{\lambda_i}{2}\right) \end{aligned} \tag{30}$$

where σ_s is the solidity of a single blade, i.e.:

$$\sigma_s = \frac{c}{\pi R} \tag{31}$$

and λ_i is the inflow ratio:

$$\lambda_i = \frac{v_i}{\Omega R} \tag{32}$$

The Ornicopter's shaft torque coefficient can be derived in the same way, and this gives:

$$C_{Q_s} = C_{T_s}\lambda_i + C_{Q0_s} - \frac{1}{16}\sigma_s C_{L_\alpha}\left(\hat{\beta}^2 + \beta_{c1}\theta_{s1} - \beta_{s1}\theta_{c1}\right) \tag{33}$$

in which $\hat{\beta}$ is the amplitude of the blade flapping motion.

References

[1] Harris, F. D., Kasper, E. F., and Iseler, L. E., "U.S. civil rotorcraft accidents, 1963 through 1997," NASA Technical Memorandum 209597, NASA, 2000.

[2] Geißler, W. and van der Wall, B. G., "Rotor without Reaction Torque, a Historical Review of H.G. Küssner's Rotorcraft Research," *66th American Helicopter Society Annual Forum*, May 2010.

[3] Geißler, W. and van der Wall, B. G., "The Flapping Propulsion Rotor, Single Rotor without Tail Rotor," *1st Asian-Australia Rotorcraft Forum*, February 2012.

[4] Savov, V. and Raikov, M., "Autorotating rotor with Ornithopter-like flapping blades," *Aeronautical Journal*, Vol. 106, No. 1061, 2002, pp. 399–409.

[5] van Holten, T., "A single rotor without reaction torque: a violation of Newton's Laws or feasible?" *28th European Rotorcraft Forum*, 2002.

[6] Torenbeek, E. and Deconinck, H., *Innovative configurations and advanced concepts for future civil aircraft: June 6-10, 2005*, Lecture series, Von Karman Institute for Fluid Dynamics, 2005.

[7] van Holten, T., Heiligers, M., and van de Waal, G. J., "The Ornicopter: A Single Rotor without Reaction Torque, Basic Principles," *24th International Congress of the Aeronautical Sciences*, 2004.

[8] van Holten, T. and Heiligers, M., "Configuration Analysis of A Torqueless Helicopter Concept," *24th International Congress of the Aeronautical Sciences*, 2004.

[9] van Holten, T., "HELICOPTER," Patent Application, 01 2004, WO 2004/002825 A1.

[10] Wan, J. and Pavel, M., "Mimicking Birds to Invent a Tailless Helicopter-the Ornicopter," *67th American Helicopter Society Annual Forum*, May 2011.

[11] Wan, J. and Pavel, M., "The Ornicopter - a tailless helicopter with active flapping blades," *The Aeronautical Journal*, Vol. 118, No. 1205, 2014, pp. 743–773.

[12] Wan, J., *Ornicopter Multidisciplinary Analyses and conceptual Design*, Ph.D. thesis, Delft University of Technology, 2014.

[13] Wan, J. and Pavel, M., "Ornicopter: a birds-like tailless helicopter," *1st Asian-Australia Rotorcraft Forum*, February 2012.

[14] Wan, J. and Pavel, M., "Stability and controllability analysis for Ornicopter," *37th European Rotorcraft Forum*, September 2011.

[15] Wan, J. and Pavel, M., "Directional handling quality assessment for Ornicopter," *38th European Rotorcraft Forum*, September 2012. ***

[16] Filippone, A., *Flight performance of fixed and rotary wing aircraft*, Elsevier Aerospace Engineering Series, Butterworth-Heinemann, 2006.

[17] Leishman, J., *Principles of Helicopter Aerodynamics*, Cambridge Aerospace Series, Cambridge University Press, 2006.

[18] Platzer, M. F., Jones, K. D., Young, J., and S. Lai, J., "Flapping wing aerodynamics: progress and challenges," *AIAA journal*, Vol. 46, No. 9, 2008, pp. 2136–2149.

[19] Byrd, R. H., Gilbert, J. C., and Nocedal, J., "A trust region method based on interior point techniques for nonlinear programming," *Mathematical Programming*, Vol. 89, No. 1, 2000, pp. 149–185.

[20] Byrd, R. H., Hribar, M. E., and Nocedal, J., "An interior point algorithm for large-scale nonlinear programming," *SIAM Journal on Optimization*, Vol. 9, No. 4, 1999, pp. 877–900.